

THE EVALUATION OF STABLE ISOTOPES
OF CARBON AND STRONTIUM AS TRACERS
FOR ESTIMATION OF CO₂ STORAGE IN
RECENT TUFA IN RIVER KRKA (CROATIA)

Qasim Jamil

Master Thesis
Jožef Stefan International Postgraduate School
Ljubljana, Slovenia

Supervisor: Prof. Dr. Sonja Lojen, Jožef Stefan Institute, Ljubljana, Slovenia
Co-Supervisor: Asst. Prof. Dr. Tea Zuliani, Jožef Stefan Institute, Ljubljana, Slovenia

Evaluation Board:

Prof. Dr. Janez Ščančar, Chair, Jožef Stefan Institute, Ljubljana, Slovenia
Dr. Neven Cukrov, Member, Institut Ruđer Bošković, Zagreb, Croatia
Asst. Prof. Dr. Tea Zuliani, Member, Jožef Stefan Institute, Ljubljana, Slovenia

MEDNARODNA PODIPLOMSKA ŠOLA JOŽEFA STEFANA
JOŽEF STEFAN INTERNATIONAL POSTGRADUATE SCHOOL



Qasim Jamil

THE EVALUATION OF STABLE ISOTOPES OF
CARBON AND STRONTIUM AS TRACERS FOR
ESTIMATION OF CO₂ STORAGE IN RECENT TUFA IN
RIVER KRKA (CROATIA)

Master Thesis

OCENA STABILNIH IZOTOPOV OGLJIKA IN
STRONCIJA KOT SLEDIL ZA OCENO SKLADIŠČENJA
CO₂ V RECENTNEM LEHNJAKU NA REKI KRKI
(HRVAŠKA)

Magistrsko delo

Supervisor: Prof. Dr. Sonja Lojen

Co-Supervisor: Asst. Prof. Dr. Tea Zuliani

Ljubljana, Slovenia, September 2021

To . . .My late father, for being my first teacher.

Acknowledgments

I would like to express my great gratitude to my supervisor, Prof. Dr. Sonja Lojen, for her guidance, advice and encouraging words during my postgraduate studies. I am sincerely grateful for her time and helpful remarks, which has improved the quality of this work.

Next, I would like to thank my co-supervisor, Dr. Tea Zuliani, for her help in developing methods and results measurements. I particularly thank Mr. Stojan Žigon for his technical support. A special thanks goes to the committee members for their valuable suggestions that helped me to improve the quality of this thesis.

No words of thanks can sum up my gratitude that I owe to my mother Naziran Bibi, who raised me in a way that encouraged my curiosity and kindly supported me to pursue my dreams. I shall be forever obliged to my elder sisters for their guidance, love and affection since my childhood. Finally, I would like to thank my wife, Khush Bakhat Rana, who has been a source of motivation and strength during moments of despair and discouragement.

Abstract

Water and tufa, along with soil and bedrock as the primary contributing sources of dissolved and particulate trace elements at seven waterfalls of the Krka river, Croatia, were investigated using geochemical and stable isotope tracers for the identification and quantification of authigenic carbonates. Terrestrial authigenic carbonate is one of the biggest global sinks of CO₂ in areas with dominant carbonate lithology. However, it has not yet been adequately quantified due to its dispersed occurrence. Moreover, the efficient identifiers of authigenic carbonate and adequate analytical tools still lack because of the complexity of natural processes involved in carbon storage. Isotopic composition of metals that co-precipitate and fractionate their isotopes during precipitation of carbonate from the river water, such as strontium (Sr), was an obvious choice as the tracer. The main aim of the study was to elaborate a methodology for identifying and quantifying authigenic carbonate as a temporal or permanent CO₂ sink in complex carbonate sediments formed in rivers.

The chemical and isotopic composition of river water and tufa ($\delta^{13}\text{C}$, $\delta^{88}\text{Sr}$, $^{87}\text{Sr}/^{86}\text{Sr}$) was analyzed. The method of Sr extraction from bedrock samples, soil, and tufa for their stable isotope analysis was optimized. Further, partition and isotope fractionation of carbon and strontium in the bedrock – water – tufa system. Authigenic carbonates in tufa were identified and quantified. Annual storage of CO₂ in tufa in the Krka river was estimated. PhreeqC programme was used to perform the geochemical modelling of solutions and determine the saturation state of water, and the ISOSOURCE programme was used to estimate the proportions of authigenic and detrital carbonate in tufa.

The study is based on the results obtained from one sampling campaign only. The obtained results depict that soil and dissolution of bedrock are the main sources of detrital Sr. The lower $\delta^{88}\text{Sr}$ value in tufa than its precipitating water evidently shows the precipitation of authigenic carbonates. Moreover, it is proved that stable Sr isotope fractionation can be used as efficient tracers for the identification and quantification of authigenic carbonate and CO₂ storage in the studied environment.

Povzetek

Vodo in lehnjak ter tla in kamninsko podlago kot primarni vir raztopljenih snovi in elementov v sledovih v sedmih slapovih reke Krke na Hrvaškem smo raziskali z uporabo geokemičnih in stabilnih izotopskih sledil za identifikacijo in količinsko opredelitev avtigenih karbonatov. Kopenski avtigeni karbonat je eden največjih ponorov CO₂ na območjih s prevladujočo karbonatno litologijo. Vendar pa zaradi razpršene pojavnosti še ni bil ustrezno količinsko opredeljen. Poleg tega še vedno primanjkuje učinkovitih identifikatorjev avtigenega karbonata in ustreznih analitičnih orodij zaradi zapletenosti naravnih procesov, povezanih s skladiščenjem ogljika. Izotopska sestava kovin, kot je stroncij (Sr), katere izotopi se med obarjanjem karbonata iz rečne vode frakcionirajo, je bila očitna izbira za sledilo. Glavni cilj študije je bil izdelati metodologijo za identifikacijo in količinsko opredelitev avtigenega karbonata kot začasnega ali trajnega ponora CO₂ v kompleksnih karbonatnih sedimentih, ki nastanejo v rekah.

Analizirana je bila kemijska in izotopska sestava rečne vode in lehnjaka ($\delta^{13}\text{C}$, $\delta^{88}\text{Sr}$, $^{87}\text{Sr}/^{86}\text{Sr}$). Optimizirana je bila metoda ekstrakcije Sr iz vzorcev kamnin, tal in lehnjaka za analizo stabilnih izotopov Sr. Nadalje je bila analizirana porazdelitev in izotopska frakcionacija ogljika in stroncija v sistemu kamnina – voda – lehnjak ter izotopska in masna bilanca Sr v sistemu voda – lehnjak. Avtigeni karbonat v lehnjaku je bil identificiran in količinsko opredeljen. Ocenjena je bila količina letno uskladiščenega CO₂ v lehnjaku v reki Krki. Za geokemijske izračune in modeliranje raztopin smo uporabili program PhreeqC, za oceno količinskih deležev avtigenega in detritičnega karbonata v lehnjaku pa program ISOSOURCE.

Študija temelji na rezultatih, dobljenih s samo enim vzorčenjem. Dobljeni rezultati kažejo, da sta tla in kamninska podlaga glavna vira Sr. Nižja vrednost $\delta^{88}\text{Sr}$ v lehnjaku kot v vodi, iz katere se je oboril s karbonatom, očitno kaže na obarjanje avtigenih karbonatov. Poleg tega je dokazano, da lahko izotopsko razmerje stabilnih izotopov Sr ($\delta^{88}\text{Sr}$) uporabimo kot sledilo za identifikacijo in količinsko opredelitev avtigenega karbonata in skladiščenja CO₂ v proučevanem okolju.

Contents

List of Figures	xv
List of Tables	xvii
Abbreviations	xix
Symbols	xxi
1 Introduction	1
1.1 Stable Isotopes as Environmental Tracers	1
1.1.1 Isotopic fractionation	2
1.1.2 The delta (δ) notation	2
1.1.3 Isotopic standards	3
1.1.4 Applications of stable isotopes	3
1.2 The Carbon Cycle	4
1.2.1 C cycling in rivers	5
1.2.1.1 Tufa	6
1.2.1.1.1 Depositional process	7
1.2.2 C isotope fractionation in rivers	8
1.2.3 Trace element partitioning	8
1.3 Non-Traditional Isotopes	9
1.3.1 Sr isotope geochemistry	10
1.4 Isotopic Standards	11
1.5 Environmental Proxies in Tufa	12
1.5.1 Stable isotope thermometer	12
2 Aims and Hypothesis	15
3 Study Area	17
4 Materials and Methods	19
4.1 Sampling Scheme and Procedures	19
4.1.1 Tufa bedrock and soil sampling	20
4.2 Isotopic Composition of Dissolved Inorganic Carbon	20
4.3 Isotopic Compositions of Hydrogen ($\delta^2\text{H}$) and Oxygen ($\delta^{18}\text{O}$) of Water	21
4.4 Chemical Analyses	21
4.4.1 X-Ray diffraction analyses	21
4.4.2 X-Ray fluorescence analysis	21
4.4.3 Analyses of sedimentary organic carbon	21
4.5 Stable Isotope Analyses of Bedrock and Tufa	22
4.6 Sr Isotope Analyses	22
4.6.1 Sample digestion for bulk samples	22

4.6.2	Sample preparation for carbonate leaching	22
4.6.3	Sample evaporation.....	23
4.6.4	Sr extraction	23
4.7	Thermodynamics Modelling and Calculations.....	23
4.8	Calcite Precipitation Rate	23
5	Results	25
5.1	Physicochemical Characteristics.....	25
5.1.1	Cations and DIC.....	26
5.2	Elemental Ratios	27
5.3	Saturation Index (SI_{calcite}) and Partial Pressure of CO_2 ($p\text{CO}_2$)	28
5.4	Stable Isotopes	28
5.4.1	Isotopic composition of river water.....	28
5.4.2	Isotopic composition of dissolved inorganic carbon (DIC) ($\delta^{13}\text{C}_{\text{DIC}}$).....	29
5.4.3	Isotopic composition of Sr in water.....	29
5.5	Tufa.....	30
5.5.1	Non-carbonate fraction	30
5.5.2	Sedimentary organic carbon (SOC)	30
5.5.3	Stable isotope composition of carbon and oxygen.....	31
5.5.4	Stable and radiogenic isotope of Strontium	31
5.6	Bedrock and Soil	32
5.6.1	Stable isotope composition of C and O.....	32
5.6.2	Sr in soil and bedrock	33
6	Discussions	37
6.1	Material Sources for Tufa Precipitation	37
6.1.1	Main source – river water	37
6.1.1.1	Dissolved inorganic carbon.....	37
6.1.1.2	Metals in water	38
6.1.2	Detrital material	38
6.2	Tufa Precipitation	39
6.2.1	C isotope variation in tufa.....	39
6.2.2	Sr in tufa.....	40
6.3	Identification and Quantification of Authigenic Carbonate.....	42
6.4	Tufa as CO_2 Sink?.....	43
7	Conclusions	45
	References	47
	Bibliography	61
	Biography	63

List of Figures

Figure 1.1: Global biogeochemical cycle of carbon (Mackenzie & Lerman, 2006b). The main carbon reservoirs are carbonate sediments, marine, land biomass and atmosphere.	5
Figure 3.1: Location of the Krka river and sampling sites.....	18
Figure 5.1: Downstream variation of (a) temperature and (b) pH.	25
Figure 5.2: Downstream variation of (a) conductivity and (b) Eh in the Krka river water.....	26
Figure 5.3: Downstream variation of (a) Ca^{2+} , (b) Mg^{2+} , (c) Sr^{2+} and (d) K^+ content in the Krka river.....	26
Figure 5.4: (a) Total alkalinity and (b) total DIC concentration downstream variation in the Krka river.	27
Figure 5.5: Variation of (a) Mg:Ca and (b) $1000 \times \text{Sr}:\text{Ca}$ molar ratios downstream the spring in the Krka river.....	27
Figure 5.6: Variation of (a) $\text{SI}_{\text{calcite}}$ and (b) $\log \text{pCO}_2$ downstream the spring in the Krka river.	28
Figure 5.7: Downstream pattern of $\delta^{18}\text{O}$ in the Krka and Zrmanja river water.	28
Figure 5.8: $\delta^{13}\text{C}$ variation in downstream of the spring of the Krka and Zrmanja rivers.	29
Figure 5.9: Downstream variation of $\delta^{88/86}\text{Sr}$ in the Krka and Zrmanja rivers.....	29
Figure 5.10: Downstream variation of non-carbonate fraction in tufa.	30
Figure 5.11: Spatial variability pattern of SOC concentration in tufa.....	31
Figure 5.12: Downstream variations in $\delta^{18}\text{O}$ and $\delta^{13}\text{C}$ values in tufa.....	31
Figure 5.13: Downstream variability in a) $^{87}\text{Sr}/^{86}\text{Sr}$ and b) $\delta^{88/86}\text{Sr}$ in tufa.....	32
Figure 5.14: $\delta^{18}\text{O}$ and $\delta^{13}\text{C}$ in soil, bedrock and tufa.....	32
Figure 5.15: $\delta^{88}\text{Sr}$ and $^{87}\text{Sr}/^{86}\text{Sr}$ in soil, bedrock and tufa.....	33
Figure 6.1: Plot of Sr versus non-carbonates in soil.....	38
Figure 6.2: Plot of $1000 \times \text{Sr}/\text{Ca}$ versus temperature in the Krka water.....	41
Figure 6.3: Rate dependence of a) $\delta^{88}\text{Sr}$ b) $\Delta^{88}\text{Sr}_{\text{t-w}}$ in tufa formation in the Krka river...	42

List of Tables

Table 1.1: Isotopes of Sr and their natural abundance.	10
Table 1.2: $\Delta^{88}\text{Sr}_{\text{carb-aq}}$ (‰) values in inorganic and biogenic calcite from various sources.	11
Table 1.3: The fractionation factors for C in the calcite - HCO_3^- system ($^{13}\alpha_{\text{cc-HCO}_3}$) and O in the calcite - water system ($^{18}\alpha_{\text{cc-w}}$).	13
Table 4.1: Coordination locations, elevations and their distance from the spring.	19
Table 5.1: Results of physico-chemical parameters in the Krka river and of chemical and isotopic analyses in the Krka and Zrmanja rivers.	34
Table 5.2: Isotopic and geochemical parameters of tufa, bedrock and soil samples from the Krka river.	35
Table 6.1: Combinations of sources for each site.	43
Table 6.2: Calculation of CO_2 storage capacity for the studied sites.	43

Abbreviations

VSMOW	... Vienna Standard Mean Ocean Water
VPDB	... Vienna Pee Dee Belemnite
IAEA	... International Atomic Energy Agency
NIST	... National Institute of Standard and Technology
DIC	... Dissolved inorganic carbon
TIMS	... Thermal ionization mass spectrometry
ICP-MS	... Inductively coupled plasma mass spectrometry
DBL	... Diffuse boundary layer
EPS	... Extracellular polymeric substances
HDPE	... High-density polyethylene
XRD	... X-ray diffraction
XRF	... X-ray fluorescence
SOC	... Sedimentary organic carbon
SI	... Saturation index
HNO ₃	... Nitric acid
HCl	... Hydrochloric acid
SIMS	... Secondary ion mass spectrometry

Symbols

α	... Isotope fractionation factor
ε	... Isotope enrichment factor
δ	... Relative isotopic composition, Delta, in per mil (‰)
ω	... Thickness of the water layer
φ	... Thickness of the DBL
$\delta^{13}\text{C}$... Carbon isotopic composition
$\delta^{18}\text{O}$... Oxygen isotopic composition
$\delta^{88}\text{Sr}$... Sr stable isotopic composition
$^{87}\text{Sr}/^{86}\text{Sr}$... Sr radiogenic isotope ratio
T	... Temperature
R	... Calcite precipitation rate
$p\text{CO}_2$... Partial pressure of carbon dioxide
ρ	... Reaction rate constant
M	... Molar concentrations

Chapter 1

Introduction

The efficient accountancy of the global carbon budget, the knowledge of carbon cycle paths and the processes that affect the hydrosphere, atmosphere, biosphere, and lithosphere system are the most important challenges in the science of global environmental changes (Tans et al., 1990; Esser et al., 2011; Cao et al., 2012). The study of the carbon cycle is necessary for a better understanding of the pathways of carbon across phase boundaries carbon (C) exchange between spheres. Climate change and global warming concerns have triggered CO₂ research. The concentration of atmospheric CO₂ is increased to 407.38±0.1 ppm in 2018 (Dlugokencky & Tans, 2019). The increase in the atmospheric CO₂ reflects roughly about half of the CO₂ in anthropogenic emission, and the other half is due to carbon sequestration in the oceans and terrestrial biosphere (Tans et al., 1990). The increasing atmospheric CO₂ concentration instigated the study of its storage.

The riverine system is essential in the global carbon cycle not only because of transportation of carbon from the terrestrial environment into the oceans and carbon sink but also it exchanges CO₂ with the environment and precipitates the carbonates in the streams. (Richey, 2005). Conventionally, there are two major carbon sinks, organic carbon and marine carbonates (Schrag et al., 2013). Lately, it was proposed that authigenic carbonate (e.g. carbonate cements, flowstone and speleothems in caves, tufa in rivers and lakes, etc.) is one of the biggest global sinks of CO₂ (Sun et al., 2014; Zhao et al., 2016). In terrestrial settings, it is highly relevant, in particular in areas with dominant carbonate lithology (Buttman & Raymond, 2011; Rassmann et al., 2016; Zhao et al., 2016). However, because of its dispersed occurrence, it has not yet been adequately quantified. Moreover, because of the complexity of natural processes involved in carbon storage, the efficient identifiers of authigenic carbonate and adequate analytical tools are still lacking (Zhao et al., 2016).

1.1 Stable Isotopes as Environmental Tracers

The natural or ambient elements e.g. C, O, Mg and Sr, widely spread on the earth's near-surface can be potentially used as environmental tracers. They provide an important tool to find the source and different dynamics of the ecosystem through their variation. Stable isotopes are used in hydrology, hydrogeology, and ecological studies as environmental tracers (Green & Taheri, 1992; Johnson et al., 2004; Michener & Lajtha, 2007).

Atoms having the same number of electrons and protons, but the different number of neutrons are isotopes. They can be denoted as ${}^m_n\text{E}$ where m is the mass number and n is the atomic number of an element E. Stable isotopes are those which do not decay or decay at such a low rate that it cannot be detected with the most up-to-date equipment.

Mass difference and physicochemical properties cause the behaviour of stable isotopes to be controlled by kinetic and vibrational energy. This leads to isotope fractionation, which is the relative partitioning of the isotopes between two substances or two phases of identical substances with different isotope ratios. The largest differences in isotopes occur amid the lightest elements.

1.1.1 Isotopic fractionation

The types of isotopic fractionation are equilibrium and kinetic fractionation.

Equilibrium fractionation is a particular case in which isotope distribution varies between phases (liquid *vs.* vapour) or chemical substances (reactant *vs.* product) or between particular molecules when no net reaction takes place (Hoefs, 2009). In such reactions, chemical equilibrium can be attained when reactants and products stay in close contact in a well-mixed and closed system where back-reaction can happen. With the greatest differences happening at the minimal temperature, the degree of the variance in initial and final masses in equilibrium reactions depends upon temperature. Heavy isotopes tend to cumulate in denser phases (Bigeleisen & Mayer, 1947).

Kinetic fractionation appears in unidirectional or incomplete reactions, and it influences the rate constant of the reaction. In this fractionation, no isotopic equilibrium can happen (Tiwari et al., 2015). Kinetic fractionation is typically associated with diffusion, evaporation, biologically mediated and dissociation reactions and redox reactions. Usually, the lighter isotopes in a reactant can react more quickly than the heavier isotopes. As a result, lighter isotopes accumulation will occur in the product. A perfect example of the kinetics isotope reactions is biological processes, where organisms use species enriched in lighter isotope due to the lower energy consumption in dissociation bond in such molecules. This results in isotope fractionation yielding an isotopically light product and isotopically heavier residual substrate. Kinetic isotope fractionation of biologically mediated processes differs in magnitude, depending upon the concentration of reactants and product, reaction rates, environmental conditions in metabolic transformation and organism species. Generally, the organism has more time in slower reaction steps, so slower reaction steps give more isotopic fractionation than the faster reaction steps (Kendall & McDonnell, 1998).

1.1.2 The delta (δ) notation

Various materials have enormously small isotopic differences, McKinney et al., (1950) used delta δ notation to express stable isotopic data of all materials except interstellar dust. It has become common practice. δ values are expressed in parts per thousand (per mil) deviations from the standard.

$$\delta \text{ ‰} = \left(\frac{R_{\text{sample}}}{R_{\text{standard}}} - 1 \right) \times 1000 \quad 1.1$$

where R is the ratio of heavier to lighter isotope abundance. R_{sample} denotes the ratio in the sample and R_{standard} ratio in the standard. A positive δ value shows that the sample has more heavy isotopes than the standard, while a negative value indicates vice versa. Typical means for the comparison of the isotopic composition of the two materials include high *vs.*

low values, heavy *vs.* light, enriched *vs.* depleted and more or less positive. Enriched *vs.* depleted is only used to clarify to which isotope the sample is enriched or depleted in. δ notation for the stable isotope of C, O and Sr are $\delta^{13}\text{C}$, $\delta^{18}\text{O}$ and $\delta^{87/86}\text{Sr}$, respectively.

The isotopic fractionation is expressed with fractionation factor (α), commonly replaced by separation/enrichment factor (ε) in recent years. In a chemical reaction, where reactants give the product, the fractionation factor (α) is described as the reactants' isotopic ratio and products' isotopic ratio.

$$\alpha_{\text{product-reactant}} = R_{\text{product}} / R_{\text{reactant}} \quad 1.2$$

where R is the ratio of heavy to light isotopes in reactant and product. The relation of the fractionation factor and the isotopic composition of two substances is:

$$\alpha_{A-B} = 1000 + \delta_A / 1000 + \delta_B \quad 1.3$$

where A and B show the reactant and product while δ_A and δ_B denote the isotopic fractionation of reactant and product, respectively. The (α) magnitude depends most importantly on temperature and many other factors. The value of the fractionation factor for equilibrium fractionation is close to 1 (e.g. $\alpha = 1.030$ shows that heavy isotopes in substance A are by 3% enriched than in substance B). As isotope fractionation has commonly small values, replacing α by ε has become a regular practice in recent years because it gives fractionation in parts per thousand alike δ values. The enrichment factor is defined as:

$$\varepsilon_{A-B} = \alpha_{A-B} - 1 \quad 1.4$$

Where ε denotes the enrichment or depletion of the product with heavy isotope compared to the reactant (e.g. +20‰ or -20‰).

1.1.3 Isotopic standards

The standard or reference material should be stable enough, pure element or chemical compound, widely available, homogeneous and its isotopic ratio should approximate the mean of natural variation for isotopic measurements. Lab or working standards, prepared individually, should be calibrated with international standards so that values can be reported internationally concerning to uniform scale. The primary reference materials for $\delta^{18}\text{O}$ and $\delta^2\text{H}$ are Vienna Standard Mean Ocean Water (VSMOW), Vienna Pee Dee Belemnite (VPDB) is for $\delta^{13}\text{C}$ and $\delta^{18}\text{O}$, $\delta^{15}\text{N}$ of Air- N_2 . International Atomic Energy Agency (IAEA, Vienna), Institute for Reference Materials and Measurements (Belgium), United States Geological Survey (USGS) and National Institute of Standards and Technology (NIST, USA) are some of the institutes, who prepare and distribute international standards and various certified isotopic reference materials like NBS-19 and VSMOW2. NIST SRM987 SrCO_3 is being used as a standard in Sr isotopic measurements.

1.1.4 Applications of stable isotopes

Naturally occurring isotopes of different elements (e.g., C, O, Mg and Sr) have been extensively applied in Earth sciences, biological and human sciences and several subdisciplines of chemistry. Based on the natural occurrence and the processes involved in these elements' precipitation, their applications in environmental sciences can be classified

into four major types thermometry, source appointment, palaeoclimatology and reaction mechanism (Clark & Fritz, 1997; Kendall & McDonnell, 1998; Sharp, 2007; Hoefs, 2009). Light elements (hydrogen, carbon, oxygen, nitrogen and sulfur) are the major bio-active components of the various compounds in the geo-, hydro- and biosphere. In the course of physicochemical processes, isotope partitioning of the same element is possible through the considerable relative mass difference between the heavy and light isotope of the element. Generally, stable isotopes are being used in hydrogeochemical studies in:

- (1) sources, sinks and mixing ratios identification of the water and solutes,
- (2) identification of the transportation processes,
- (3) identification of the transformation processes,
- (4) characterization of the flow paths and
- (5) biological and geochemical cycle assessment of the elements within an ecosystem.

Stable isotope techniques are often used along with measurements of major and minor elements and judicious amounts of hydrologic data to test hypothesis about hydrologic and geochemical mechanisms and also provide input for mass-balance calculations and quantitative constraints on reaction progress (Kendall & McDonnell, 1998).

1.2 The Carbon Cycle

Carbon is the primary constituent of the terrestrial and marine hydrosphere, biosphere and atmosphere. It is an integral part of organic and inorganic matter, an essential component of metabolism in organisms, and critical to the chemical weathering of rocks (Mackenzie & Lerman, 2006). The global biogeochemical cycle is shown in Figure 1.1. A conceptual biogeochemical model that reflects geological and physicochemical processes of carbon transfer between different reservoirs is a vital tool to elaborate the storage, flow and transformations of carbon.

Chemical weathering of sedimentary, photosynthesis and crystalline silicate rocks at the Earth's surface controls the global atmospheric CO₂ concentration. Rock weathering absorbs CO₂ primarily from the atmosphere or soil and yields aqueous carbonate and bicarbonate ions, which are then carried away by the river to the oceans (Sun et al., 2010). In most cases, weathering occurs by reaction with dissolved C, not directly with CO₂ from the atmosphere. The carbonate system is the most important in low-temperature geochemistry. It includes the species of carbon in gaseous (i.e. CO₂ (g)), aqueous (i.e. dissolved CO₂, carbonate and bicarbonate ions) and solid carbonate, most commonly CaCO₃ or MgCO₃ phases (Yan et al., 2020). The formation of carbonate rocks and silicate rock weathering plays a vital role in atmospheric CO₂ consumption and release. (Gaillardet et al., 1999; Oliva et al., 2003). The carbon isotope composition ($\delta^{13}\text{C}$) value is source dependent and conspicuously distinct in terrestrial carbonates from that of carbonate bedrock formed in the marine environment. Therefore, the $\delta^{13}\text{C}$ value has been widely used in earth sciences, paleoclimate reconstruction (e.g. Dorale et al., 1998; Zachos et al., 2001) and also as a tracer of carbon flow in natural reservoirs (e.g. Quarry et al., 1992; Ehleringer et al., 2000; Zavadlav et al., 2012, 2013).

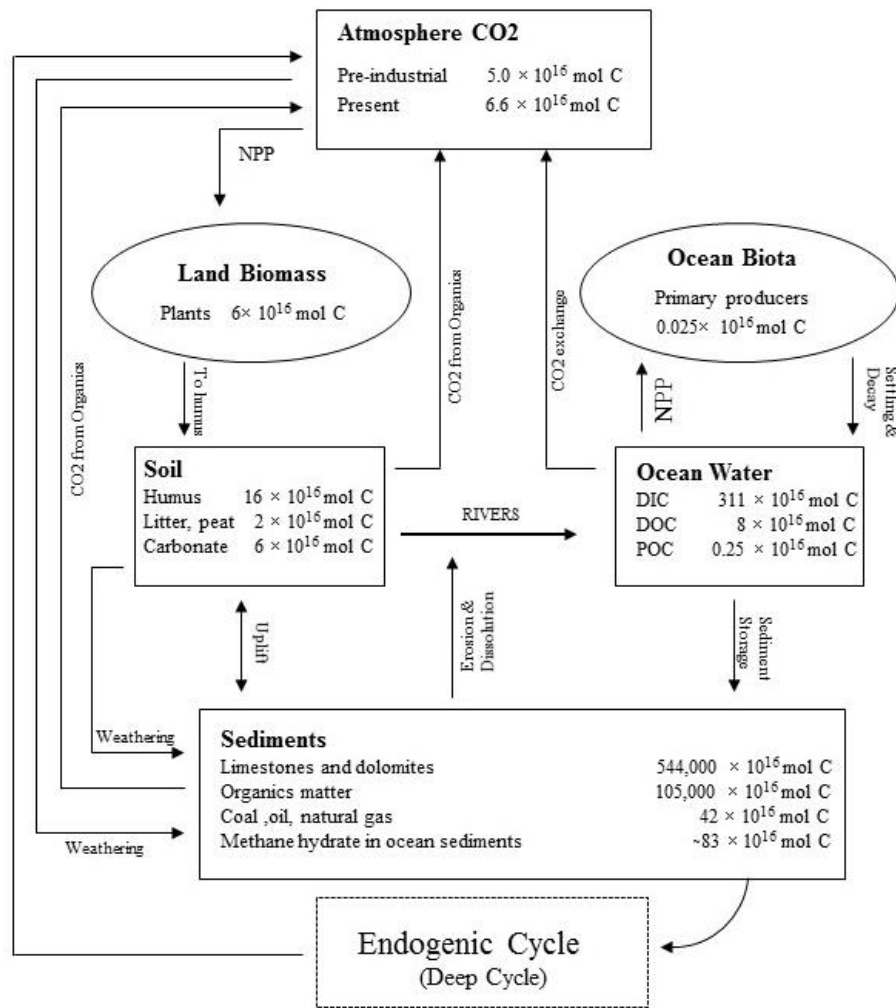


Figure 1.1: Global biogeochemical cycle of carbon (Mackenzie & Lerman, 2006b). The main carbon reservoirs are carbonate sediments, marine, land biomass and atmosphere.

Any carbonate mineral can be termed authigenic minerals, precipitated inorganically *in-situ* either from the sediment pore water or at the sediment-water interface. At very high supersaturation, homogenous or heterogenous nucleation can occur in the water, not only on substrates (hard or soft). Authigenic carbonates precipitate when alkalinity is produced during the diagenesis of organic matter, which results in the supersaturation with respect to carbonate minerals in recent oceans (Schrag et al., 2013). Authigenic carbonates, as a chemical precipitate, record the ambient conditions at the time of its precipitation and at the locus of precipitation – the conditions in the microenvironment where the precipitation takes place can be very different from the conditions in the bulk solution (river) from which the CaCO_3 is precipitated (Zhao et al., 2016)

1.2.1 C cycling in rivers

Rivers act as reactive conduits, which connect the continental and oceanic C cycles (Cole et al., 2007). Studies of in-stream metabolism, gas exchange (Raymond et al., 2013, Hotchkiss et al., 2015), and sediment dynamics (Wohl et al., 2017) reveal that rivers are an active component of the global carbon cycles, rather than neutral pipes, and rivers form

and the process can significantly affect the terrestrial derived carbon partitioning among the geosphere, atmosphere and oceans (Aufdenkampe et al., 2011).

The important carbon sources in rivers are geological processes (weathering), aquatic photosynthesis and CO₂ exchange with the atmosphere. To constrain the sources, and solute and water cycling in river system, geochemical and hydrological analyses serves as a good tool to evaluate riverine water hydrobiogeochemical state. The riverine carbon consists of particulate and dissolved inorganic and organic carbon. Generally, the dissolved inorganic carbon (DIC) is the primary component in the river. The DIC is subjected to several in-stream processes which alter its carbon isotopic composition. Photosynthesis in the water column preferentially selects the lighter carbon, thus enriching the remaining DIC with ¹³C, while during respiration lighter carbon is added to the pool, resulting in lower ¹³C_{DIC} values. The third process, exchange with the atmosphere, involves equilibration between gaseous CO₂ and DIC. Although temperature-dependant, the isotopic fractionation between atmospheric CO₂ with ¹³C value of -7.7 ‰ (Schulte et al., 2011) and aqueous CO₂ is about +8 ‰ (Mook et al., 1974). Thus, atmospherically equilibrated DIC would yield ¹³C value of 0 ‰.

CO₂ outgassing from inland water takes place extensively in the surface water environment termed as CO₂ evasion, and it plays a significant role in the terrestrial carbon cycle (Cole et al., 2007; Raymond et al., 2013) and calcite precipitation (Dreybrodt, 2019). Dreybrodt et al. (2019) found that two types of outgassing of CO₂ occur, precipitation controlled outgassing and diffusion associated degassing, from CaCO₃ precipitation in H₂O – CO₂ system. Precipitation-controlled CO₂ outgassing is when one molecule of CaCO₃ precipitated, one molecule of CO₂ produced and escapes from dehydration and dihydroxylation of HCO₃⁻. The diffusion-associated outgassing has no significant effect on CaCO₃ precipitation, as long as the supersaturation is high. But research of tufa revealed that the CaCO₃ precipitation requires high supersaturation (upto 10 times), while the CO₂ continuously degasses from the water surface without precipitation, and in such case the degassing is not negligible (Zavadlav et al., 2017 and references therein). Yan et al. (2020) studied the non-equilibrium fractionation of carbon isotope, and his study reveals that travertine and speleothem growth from supersaturated solution drives the disequilibrium carbon isotope fractionation between CO₂ and HCO₃⁻. The kinetic isotope effect dominates in dehydration and dihydroxylation of HCO₃⁻ during isotope fractionation between CO₂ and HCO₃⁻ (Guo, 2008).

Investigation of stable isotope composition in tufa deposits shows cyclic seasonal variations in δ¹³C values of dissolved inorganic carbon (DIC) in groundwater, caused by the seasonal variations of temperature and precipitation that govern the primary production and vegetation growth, which in turn control the release of biogenic CO₂ into the water. Another important source of DIC is the dissolution of bedrock (aquifer) which also depends upon the temperature, the amount of water and the concentration of DIC accumulated in the surface discharge and soil. The atmosphere is usually a negligible CO₂ source of DIC in areas with a lot of vegetation. It is also influenced by the CO₂ degassing from water and temperature dependant processes (Matsuoka et al., 2001; Andrews, 2006).

1.2.1.1 Tufa

Water flowing in surface and groundwater in areas with dominant carbonate bedrock is usually saturated with respect to calcite. When supersaturated with respect to CaCO₃, water precipitates calcium carbonate inorganically or microbiologically and/or degasses carbon dioxide (Horvatinčić et al., 2003, Chen et al., 2004). Calcareous precipitates that form in springs, rivers or lakes at ambient temperature are called tufa. It can form

spectacular terraces, cascades and dams in rivers, transforming the river flow into a series of lotic and lentic environments. It can also be present as loosely bound or compact coatings or laminated crusts or as stratified lacustrine sediment in different, most commonly, karst regions of the world. (Pentecost, 2005; Pedley, 2014 and references therein).

The precipitation of calcite has a significant effect on the hydrochemical evolution of the riverine system because CO₂ in considerable amount is emitted to the atmosphere directly from the water (Buttman & Raymond, 2011; Raymond et al., 2013; Yan et al., 2020) and during the precipitation process (Horvatinčić et al., 2003; Chen et al., 2004). The term travertine is sometimes also used in tufa, although it is referred to as carbonate sinter deposited in hydrothermal systems (hot springs) (Ford & Pedley, 1996).

Tufa deposits can give answers to many research questions about the terrestrial record, origin, landscape developments, palaeoclimatology, tectonics and astrobiology (Capezzuoli et al., 2014a). An enhanced understanding of the formation process and deposition settings are required to use tufa deposits for these queries. Tufa as a CO₂ sink may be relatively small on a global scale but can play a significant role locally in karstic regions.

1.2.1.1.1 Depositional process

Carbonate precipitation occurs as a result of a variety of different processes. However, tufa formation by abiotic processes has been generally an identified process. Calcium and bicarbonate ions can be dissolved by percolating water whenever they flow across the soil horizon. Usually, the CO₂ level is high in the soil horizon because of biogenic activities, e.g. decomposition of organic matter, respiration of microbial communities, etc. Hence, this water can be easily saturated or supersaturated with calcium carbonate (Horvatinčić et al., 2003). After passing the soil horizon, the infiltrating water is usually supersaturated with CO₂; if such water flows into the river as surface discharge, then it contributes dissolved and biogenic CO₂ to the river water. The availability of Ca in the soil may vary, depending on the minerals composition of the soil and bedrock – saturation with respect to CaCO₃ usually occurs in the aquifer when this CO₂-rich water dissolves the bedrock.

After its underground flow, it discharges in springs or diffuses discharge directly into the river. A variety of processes leads it to the release of CO₂ gas, such as variation in the water turbulence, temperature, pressure and mixing with water with different calcium carbonate concentrations and precipitation of CaCO₃ (Riding, 1979; Marker, 1988; Ford & Pedley, 1996; Andrews, 2006). Precipitation of calcite from water can be simply expressed as:



Thus, the tufa depositional rate depends upon these abiotic/biogenic processes. The depositional rate of tufa, for example, in fossil deposits ranges from 0.32 – 42 mm/year (Weijermars et al., 1986; Heiman & Sass, 1989; Andrews et al., 2000; Peña et al., 2000). In recent tufa deposits, direct measurements revealed deposition rate in the same range of values, e.g., the average growth rate of tufa at Skradinski Buk area, Krka National Park, Croatia, is 5.771 mm/year (Marić et al., 2020), mean depositional rate recorded in the Piedra River from November 1999 to September 2012 is 7.86 mm/year (Arenas et al., 2014) and in the area of Natural Park, the value is 7.52 mm/year (Vázquez-Urbez et al., 2010). Substrate topography, a corresponding type of vegetation, water hydrochemistry and particularly, microbes present there play a significant role in the depositional facies and potential for preservation.

1.2.2 C isotope fractionation in rivers

Carbon exists on Earth has two stable (^{12}C and ^{13}C) and one radioactive isotope (^{14}C). the abundance of ^{12}C and ^{13}C is 98.89% and 1.108%, respectively. ^{14}C is produced by the interaction of thermal neutrons and nitrogen atoms in the upper atmosphere. The ^{14}C has a half life for the decay 5,730 years and can be used in the determining the objects' age having a biological origin upto about 50,000 years of age (Arnold & Libby, 1949). The stable isotope ratio $^{12}\text{C}/^{13}\text{C}$ has been widely used as discussed earlier.

The sources of riverine carbon are mentioned earlier, where stable isotopes can help to constrain the inputs from the dissolution of various minerals and rock types. The C isotopic composition of DIC is function of abundance of the species CO_2 , HCO_3^- , and CO_3^{2-} (Schulte et al., 2011). The seasonal changes in $\delta^{13}\text{C}$ DIC occur when water is exposed to atmospheric CO_2 of high ^{13}C due to the natural ventilation, which increases in winter, instead of inducing outgassing, removes CO_2 of low ^{13}C from the water. It significantly impacts the seasonal pattern of $\delta^{13}\text{C}$ (Hori et al., 2008).

Stable isotopes of carbon and oxygen ($\delta^{13}\text{C}$ and $\delta^{18}\text{O}$ values) are more often used tracer of authigenic carbonates. However, in environments with multiple C sources and changing redox conditions, such as organic-rich carbonaceous sediments, the isotopic signatures of dissolved carbonate vary not only because of different C sources, but also because of many diagenetic processes that remove or add dissolved inorganic C (DIC) from/to the interstitial solution. Because of different C isotopic fractionation, these processes (e.g. limestone dissolution, carbonate precipitation, decomposition of organic matter, methanogenesis or methane oxidation) may change the isotopic composition of DIC in opposite directions. Thus, for unambiguous quantification and identification, additional identifiers of authigenic carbonates in freshwater sediments from carbonaceous settings are essential. Isotope composition of metals that co-precipitated and fractionate their isotopes during precipitation of carbonate from the river water, non-traditional isotopes of strontium (Sr), seems to be an obvious choice.

1.2.3 Trace element partitioning

Aquatic sediments serve as reservoirs of trace elements. However, due to biogeochemical processes, remobilization can occur (Ouyang et al., 2006). In natural water systems, metals associated with inorganic and organic matter through bioavailable complexes formation, adsorption and from pollution accumulate in sediments (Cukrov et al., 2013). The trace elements (Mg, Sr), divalent cations, have the ability to substitute the Ca^{2+} in the calcite crystal structure. The incorporation of trace elements (Sr^{2+}) mainly depends on the calcite precipitation rate and temperature in the inorganic calcite formation (Lorens, 1981; Huang & Fairchild, 2001; Tang et al., 2008a). Tufa deposits have been extensively investigated for paleoclimate and palaeoenvironmental reconstruction using C and O isotopic records as well as geochemical proxies (Mg/Ca, Sr/Ca) (Ihlenfeld et al., 2003; Lojen et al., 2004; Andrews, 2006; Brasier et al., 2010; Zavadlav et al., 2017). Ihlenfeld et al. (2003) showed that temperature derived from Mg/Ca strongly deviates from the measured temperature in recent tufa deposits. Studies have shown that microbial communities affect the incorporation of these trace elements in the tufa formation (Rogerson et al., 2008, 2014; Saunders et al., 2014; Ritter et al., 2018).

Biological/biotic processes and macrophytes presence along with heterotrophic bacteria, cyanobacteria and algae can strongly affect the precipitation of calcium carbonates (Rogerson et al., 2008; Capezzuoli et al., 2014; Saunders et al., 2014; Zhu & Dittrich, 2016;

Ritter et al., 2018). Biofilms are immensely present in tufa depositional systems, and their effective role in tufa formation is investigated in many studies (Merz-Preiß & Riding, 1999; Shiraishi et al., 2008; Arp et al., 2010; Rogerson et al., 2014; Pedley, 2014). Extracellular polymeric substances (EPS) present in biofilms chelates Ca^{2+} over Mg^{2+} result in the calcium-enriched microenvironment around the EPS molecules and yield low $(\text{Mg}/\text{Ca})_{\text{calcite}}$ as compare to the expected $(\text{Mg}/\text{Ca})_{\text{solution}}$ ratio (Rogerson et al., 2008; Saunders et al., 2014). Extracellular polymeric substances (EPS) in biofilms influence the distribution by binding the divalent cations through a negatively charged functional group (Dupraz et al., 2009; Decho, 2010;). Rogerson et al. (2008) investigated that biofilms and EPS have the capability to accumulate the Ca^{2+} and other divalent cations Mg^{2+} and Sr^{2+} by chelation process. Microbial communities can strongly affect the trace element partitioning into calcium carbonate deposits. This provides a better understanding of biological influences on tufa precipitation.

The substitution degree of trace elements in calcite precipitation is generally expressed as distribution coefficient, which is calculated as (Saunders et al., 2014):

$$D_X = \frac{(X/\text{Ca})_{\text{carbonate}}}{(X/\text{Ca})_{\text{water}}}$$

where X is the trace element, and D_X denotes the distribution coefficient. D_X depends on temperature, precipitation rate and microbial communities.

1.3 Non-Traditional Isotopes

Isotopes of elements other than H, C, O, N and S, are known as non-traditional isotopes.

In environmental geochemistry, isotopes signatures of elements (e.g., C, O, Mg and Sr) are being vastly used as environmental tracers to study the climate due to the exceptional attribution of variation in their natural or anthropogenically induced abundance. The isotope fractionation provides information about the paleoenvironment (Hoefs, 2009).

ICP MS technique, Thermal Ionization Mass Spectrometry (TIMS) or Secondary Ion Mass Spectrometry (SIMS) are being used to measure the isotopic variability of the elements, in contrast to “traditional” isotopes those are analysed using a gas source magnetic sector mass spectrometry (IRMS) (Teng et al., 2017).

Metal stable isotopes, Si and Cl isotopes, etc., are usually referred to as non-traditional isotopes. Isotopic analyses of non-traditional isotopes have been started later than the traditional isotopes. Although the development on Li isotope geochemistry based on TIMS was made in the 1980s (Chan, 1987), the introduction of new instrumentation, Multicollector ICP-MS in 1992, by coupling of multi-collector detector array to an ICP-MS (Douthitt, 2008), has initiated the new research field of cosmo and geochemistry. Afterwards, precise measurements of the isotopes of light and heavy elements (e.g. Mg and U) can be done sufficiently precisely to trace the natural variations.

Non-traditional stable isotopes have various distinguishing characteristics over traditional stable isotopes. 1) these elements occur in a large range from extremely volatile to refractory; 2) the concentration of most of these elements, trace elements, in different geological reservoirs vary significantly; 3) several elements are biologically active; 4) most of them are redox-sensitive; 5) the atomic numbers of the several elements are high, and their number of a stable isotope is greater than two (Teng et al., 2017). Due to these special traits, these isotopes have become the unique tracers of various biological, geological and cosmochemical processes. Studies show that speciation, volatility, relative mass difference and biological sensitivity effects the non-traditional stable isotopes’ variation (Teng et al.,

2017). The stable isotope of Sr is evaluated in this study as a tracer to estimate the CO₂ storage in the tufa. The isotope geochemistry of Sr is as follows.

1.3.1 Sr isotope geochemistry

Strontium, an alkaline earth element, has four stable isotopes (Table 1.1). ⁸⁷Sr is the radiogenic isotope and a decay product of β emitting isotope ⁸⁷Rb, which has a half-life of 48 billion years (Banner, 2004). Strontium isotopes ⁸⁷Sr/⁸⁶Sr have been used as environmental tracers in hydrologic studies (e.g. Capo et al., 1998; Shand et al., 2009). The different Rb and Sr ratio in rocks gives different ⁸⁷Sr/⁸⁶Sr ratios in different ages, which is extensively used to differentiate silicate and carbonate weathering and their sources (Palmer & Edmond, 1992; Brennan et al., 2014), study geochemical and sedimentology attributes in Neoproterozoic cap carbonates (Liu et al., 2013, 2014, 2018), Sr cycling in the marine ecosystem (Mokadem et al., 2015), fingerprinting water sources (Zieliński et al., 2017), clastic and karst aquifer investigations (Tchaikovskiy et al., 2019), etc.

Table 1.1: Isotopes of Sr and their natural abundance.

Isotope	Abundance (%)
⁸⁴ Sr	0.56
⁸⁶ Sr	9.86
⁸⁷ Sr	7.00
⁸⁸ Sr	82.58

With the advancement in instruments, MC-ICP-MS and TIMS, and analytical methods, high precision $\delta^{88/86}\text{Sr}$ ratio analysis made it easy to measure little variability in it in the terrestrial and marine environment (Halicz et al., 2008; Chao et al., 2013, 2015), and broaden its applications in water sources investigations (Fietzke & Eisenhauer, 2006; Stevenson et al., 2014; Stevenson et al., 2018; Pearce et al., 2015; Fruchter et al., 2017; Shalev et al., 2017), paleothermometry, pedogenesis, Sr oceanic budget and biomineralization (Fietzke & Eisenhauer, 2006; Shalev et al., 2013). The relative invariability in Sr isotope ratio $\delta^{88/86}\text{Sr} = 8.375209$ is due to its smaller relative mass difference, and it has been used for instrumental fractionations calibration for high precision isotopic analysis of Sr (Teng et al., 2017).

δ notation is used to report stable Sr isotopic compositions:

$$\delta^{88}\text{Sr} \text{ ‰} = \left\{ \frac{{}^{88}\text{Sr}/{}^{86}\text{Sr}_{\text{sample}}}{{}^{88}\text{Sr}/{}^{86}\text{Sr}_{\text{standard}}} - 1 \right\} \times 1000 \quad 1.6$$

Stable Sr isotopic compositions have been assessed using both MC-ICP-MS and TIMS. Different methods are used in previous Sr investigations, which indicates that measurement using double spikes TIMS (Krabbenhoft et al., 2009) was highly accurate and precise, along with double spike MC-ICP-MS (Shalev et al., 2013) and standard-sample bracketing MC-ICP-MS (Fietzke & Eisenhauer, 2006; Charlier et al., 2012; Ma et al., 2013).

The biogenic and inorganic marine carbonate tends to have lighter $\delta^{88}\text{Sr}$ than the seawater from where precipitation occurred (Stevenson et al., 2010; Böhm et al., 2012; Shalev et al., 2013; 2017), which is $0.387 \pm 0.002 \text{ ‰}$ (Shalev et al., 2013). In global rivers, the $\delta^{88}\text{Sr}$ values were reported for Europe: 0.175-0.417 ‰, Asia: 0.260 – 0.397, Africa: 0.236-0.283, North and South America: 0.256-0.354 ‰ and Volcanic Islands: 0.126-0.566 with an

average of 0.32 ± 0.08 ‰ (Krabbenhöft et al., 2010; Pearce et al., 2015; Shalev et al., 2017).

As discussed above, the continental carbonates exhibit considerably lower $\delta^{88}\text{Sr}$ values than its precipitating water. Therefore, the $\delta^{88}\text{Sr}$ value is an efficient tool for identifying and quantifying the authigenic carbonates in the rivers. Moreover, the presence of the authigenic carbonate can also be confirmed with lower $\delta^{88}\text{Sr}$ values compared to that from the bedrock carbonates. Furthermore, few experimental studies have been performed to understand the effects of several parameters (T, R (precipitation rate) and pH) on Sr isotope fractionation ($\delta^{88}\text{Sr}$) during dissolution and precipitation of carbonates (Böhm et al., 2012). These studies reveal that T and R strongly affect the Sr isotope fractionation ($\delta^{88}\text{Sr}$) (Böhm et al., 2012; AlKhatib & Eisenhauer, 2017; Fruchter et al., 2017). Seemingly, temperature and the precipitation rate control the Sr isotopic fractionation, where higher rates increase the Sr isotope fractionation during kinetically controlled calcite precipitation (Böhm et al., 2012; AlKhatib & Eisenhauer, 2017).

Table 1.2: $\Delta^{88}\text{Sr}_{\text{carb-aq}}$ (‰) values in inorganic and biogenic calcite from various sources.

CaCO ₃	Sample	Average $\Delta^{88}\text{Sr}$ (‰)	2SD	n	Reference
Inorganic calcite	Speleothems and tufa	-0.164	0.096	17	Liu et al., 2017); Shalev et al., 2017
	Lacustrine primary calcite	-0.225	0.055	18	Fruchter et al., 2017
	Laboratory experiment	-0.244	0.120	42	Böhm et al., 2012; AlKhatib & Eisenhauer, 2017
Inorganic aragonite	Laboratory experiments	-0.175	0.044	9	Fruchter et al., 2016
Biogenic calcite	Brachiopods	-0.210	0.017	13	Vollstaedt et al., 2014
	Coccolithophores	-0.209	0.240	10	Stevenson et al., 2014
Biogenic aragonite	Scleractinian corals	-0.194	0.030	68	Raddatz et al., 2013; Fruchter et al., 2016
	Gastropods	0.211	0.027	5	Fruchter et al., 2017

The Sr stable isotope fractionation between carbonates and water $\Delta^{88}\text{Sr}_{\text{carb-w}}$ (defined as $\delta^{88}\text{Sr}_{\text{carbonate}} - \delta^{88}\text{Sr}_{\text{water}}$) from different carbonates depositional environments show an average $\delta^{88/86}\text{Sr}$ of -0.21 ± 0.10 ‰ in Table 1.2.

1.4 Isotopic Standards

All the analytical measurements have an inherent uncertainty. To mitigate this measurement uncertainty, standards are used. The standard or reference material should be stable enough, pure element or chemical compound, widely available, homogeneous and its isotopic ratio should approximate the mean of natural variation for isotopic measurements. Lab or working standards, prepared individually, should be calibrated with international standards so that values can be reported internationally concerning to uniform scale. The primary reference materials for $\delta^{18}\text{O}$ and $\delta^2\text{H}$ are Vienna Standard Mean

Ocean Water (VSMOW), Vienna Pee Dee Belemnite (VPDB) is for $\delta^{13}\text{C}$ and $\delta^{18}\text{O}$, $\delta^{15}\text{N}$ of Air- N_2 . International Atomic Energy Agency (IAEA, Vienna), Institute for Reference Materials and Measurements (Belgium), United States Geological Survey (USGS) and National Institute of Standards and Technology (NIST, USA) are some of the institutes, who prepare and distribute international standards and various certified isotopic reference materials like NBS-19 and VSMOW2. NIST SRM987 SrCO_3 is being used as a standard in Sr isotopic measurements.

1.5 Environmental Proxies in Tufa

Tufas – continental carbonate deposits – have been growingly becoming important as geochemical archives. Like speleothems and lake sediments, tufas have information about climatic and environmental conditions changes during their precipitation (Andrews et al., 1994; Ihlenfeld et al., 2003; Lojen et al., 2004, 2009; Andrews & Brasier, 2005; Dabkowski et al., 2012; Wang et al., 2014; Zavadlav et al., 2017). In tufas, stable isotopes ($^{13}\text{C}/^{12}\text{C}$ and $^{18}\text{O}/^{16}\text{O}$) and trace elements (Ca, Mg and Sr) carry information in their elemental composition and temperature of the mother solution, from where paleoclimate and paleoenvironmental conditions, hydrological conditions, and vegetation cover can be interpreted (e.g. Matsuoka et al., 2001; Ihlenfeld et al., 2003; Kano et al., 2003; Lojen et al., 2004, 2009; Andrews, 2006; Kawai et al., 2006; Hori et al., 2008; Dabkowski et al., 2012; Yan et al., 2012). Freshwater tufas are widely regarded as a potential indicator of environmental conditions at the time of their deposition (Pazdur et al., 1988; Andrews et al., 1997; Horvatinčić et al., 2000; Matsuoka et al., 2001; Ihlenfeld et al., 2003; Kano et al., 2003; Andrews, 2006; Dabkowski et al., 2012; Osácar et al., 2013; Arenas et al., 2014). It can be found in several studies that paleoclimate reconstruction from tufa can be tendentious due to the anthropogenic pollution of rivers (e.g. Leybourne et al., 2009; Lojen et al., 2009; Brasier et al., 2010). Knowledge of the chemical and physical processes taking place during tufa formation is required to interpret the stable isotope signals from the tufa. The temperature dependence of cation partitioning (e.g. Mg, Sr) in carbonate precipitation and solution is expected on theoretical grounds (Urey, 1947; Usdowski et al., 1979; Huang & Fairchild, 2001; Saulnier et al., 2012; Watkins et al., 2013, 2014; Zavadlav et al., 2017). However, biological processes are associated with tufa formation, and biofilms play a major part in trace element partitioning (Emeis et al., 1987; Pedley, 1992; Merz-Preiß & Riding, 1999b; Arp et al., 2001; Bisset et al., 2008; Shiraishi et al., 2008; Rogerson et al., 2008, 2014; Saunders et al., 2014). Biologically influenced calcite precipitation's deviation from the equilibrium between water and the precipitate is necessary to determine to get the paleoenvironmental information (Rogerson et al., 2014; Ritter et al., 2018).

1.5.1 Stable isotope thermometer

Theoretically, temperature estimation is possible if equilibrium conditions are attained during mineral formation. Equilibrium temperature can be determined by analysing any two phases existing together, which defines the isotope fractionation. On the contrary, it is not easy to prove the equilibrium in practice (Valley, 2001). The isotopic composition of carbon and oxygen of the calcite precipitate depends on the (a) isotope composition of the parent solution and (b) isotope fractionation between different species associated with the calcite precipitation process. The $\delta^{18}\text{O}$ values of precipitated calcite rely on the $\delta^{18}\text{O}$ values of water that constitute the main source of oxygen atoms, whereas the bicarbonates constitute the main reservoir of carbon atoms (in the pH range 7.5 to 8.5).

Several papers have been published since the late 1960s, which deal with both experimental and theoretical determination of equilibrium isotope fractionation in various species and phases involved in the precipitation of calcite (Polag et al., 2010). The relation between temperature and fractionation factor can be presented in the form of a basic quadratic equation (Polag et al., 2010):

$$10^3 \ln \alpha_{\text{product-reactant}} = aT^2 + bT + c \quad 1.7$$

Where α shows the fractionation factor and a, b and c are system-specific constants that can be obtained by calibrating the calculated parameters (e.g. $\delta^{18}\text{O}$ of calcite and water T) with fitting. In the calcite (cc) – HCO_3^- system, the corresponding factor in the case of $\delta^{13}\text{C}$ is $^{13}\alpha_{\text{cc-HCO}_3}$ (designation after (Polag et al., 2010), or, as a more explanatory value and isotopic enrichment factor $^{13}\varepsilon_{\text{cc-HCO}_3}$ with $\varepsilon = (\alpha - 1) \times 1000 \text{ ‰}$. The enrichment factor for $\delta^{18}\text{O}$ in the calcite (cc) – water (w) system is shown as $^{18}\varepsilon_{\text{cc-w}}$.

Isotopic fractionation can be measured in laboratory experiments (Kim & O’Neil, 1997; Dietzel et al., 2009) or natural system in geochemical equilibrium (e.g., Coplen, 2007). Over the years, developments were made on various techniques for the temperature dependence measurement of fractionation enrichment $^{13}\varepsilon_{\text{cc-HCO}_3}$ and $^{18}\varepsilon_{\text{cc-w}}$, and a vast variation in the published temperature dependence of fractionation factors featured a problem based on differences in empirical data treatment and experimental setups. The experiments show variation in isotopic fractionation factors even under similar conditions (Romanek et al., 1992; Dietzel et al., 2009; Watkins et al., 2013). Furthermore, the fractionation factor differs with temperature, and it is likely that due to its carbonate precipitation rate dependence (Feng et al., 2012; Fohlmeister et al., 2018). In calcite–water relation studies, the most often used equilibrium fractionation factors are stated below in Table 1.3.

Table 1.3: The fractionation factors for C in the calcite - HCO_3^- system ($^{13}\alpha_{\text{cc-HCO}_3}$) and O in the calcite – water system ($^{18}\alpha_{\text{cc-w}}$).

Author	Equilibrium equation
Deines et al. (1974)	$10 \cdot \ln ^{13}\alpha_{\text{cc-HCO}_3} = 0.095 \times 10^6 / T(\text{K})^2 + 0.90$
Mook (2000)	$10^3 \cdot \ln ^{13}\alpha_{\text{cc-HCO}_3} = - 4.23 \times 10^3 / T(\text{K}) + 15.10$
O’Neil et al. (1969)	$10^3 \cdot \ln ^{18}\alpha_{\text{cc-w}} = 2.78 \times 10^6 / T(\text{K})^2 - 3.39$
Friedman and O’Neil (1977)	$10^3 \cdot \ln ^{18}\alpha_{\text{cc-w}} = 2.78 \times 10^6 / T(\text{K})^2 - 2.89$
Kim and O’Neil (1997)	$10^3 \cdot \ln ^{18}\alpha_{\text{cc-w}} = 18.03 \times 10^3 / T(\text{K}) - 32.42$
Mook (2000)	$10^3 \cdot \ln ^{18}\alpha_{\text{cc-w}} = 19.668 \times 10^3 / T(\text{K}) - 37.32$
Coplen (2007)	$10^3 \cdot \ln ^{18}\alpha_{\text{cc-w}} = 17.4 \times 10^3 / T(\text{K}) - 28.6$
Daëron et al. (2019)	$10^3 \cdot \ln ^{18}\alpha_{\text{cc-w}} = 17.57 \times 10^3 / T(\text{K}) - 29.13$

Chapter 2

Aims and Hypothesis

The purpose of the thesis is to elaborate towards a methodology for the identification and quantification of authigenic carbonate as a temporal or permanent CO₂ sink in complex carbonate sediments formed in rivers. Therefore, we aim to test and validate the non-traditional stable isotopes of Sr as identifiers of authigenic carbonates in a complex multiphase material-tufa precipitated from the Krka river in the karst environment in the Outer Dinarides in central Dalmatia (Croatia). The objectives of the thesis are:

1. Analysis of the chemical and isotopic composition of river water and tufa (relevant isotopic parameters (such as $\delta^{18}\text{O}$), chemical composition, mineral composition of tufa, concentration, and isotopic composition of sedimentary organic carbon) ($\delta^{13}\text{C}$, $\delta^{87}\text{Sr}$, $^{87}\text{Sr}/^{86}\text{Sr}$),
2. Optimization of the method of extraction of Sr from bedrock samples and tufa for their stable isotope analysis,
3. Analysis of partitioning and isotope fractionation of carbon and strontium in the bedrock – water – tufa system,
4. Identification and quantification of authigenic carbonate in tufa,
5. Estimation of annual storage of CO₂ in tufa in the Krka river.

Based on the literature data, we hypothesize that stable Sr isotopic fractionation is systematic and large enough to be proven as a useful tracer for source identification and quantification of authigenic carbonate in the studied environment.

Chapter 3

Study Area

The study area is described in detail by Cukrov et al. (2008, 2013); Lojen et al. (2009). The Krka river is a groundwater-fed and medium-sized, 75 km long stream in the Dalmatian karst area draining carbonate terrains. The spring is situated close to the Knin town with a continental environment, whereas the estuary is situated in the Mediterranean area. It gets a significant fraction of water from diffuse subsurface recharge (Lojen et al., 2004, 2009; Cukrov et al., 2008, 2013; Bonacci et al., 2017). The whole catchment region's topographical settings comprise limestone and dolomites of the Cretaceous and Palaeogene age with the patches of siliciclastic sediments and flysch (Mamužić, 1971). The hydrogeological drainage area of the Krka is almost 2427 km² (Bonacci et al., 2006).

The discharge at Skradinski buk waterfalls ranges from 5 to 476 m³s⁻¹, with an average value of 51.3 m³s⁻¹ (Bonacci et al., 2017). The continuous recharge of dissolved inorganic carbon-rich groundwater primarily of biogenic origin constitutes the ideal conditions for tufa formation. The Krka river is one of the largest tufa barrier systems in Europe (Bonacci et al., 2006). A previous study (Lojen et al., 2004) depicts that the stream water is supersaturated with calcite and is degassing CO₂ along its whole 50 km course except during high water events and the extensive tufa, which is found in the riverbed, formed under non-equilibrium conditions. The various tufa barriers distinguished the river precipitated in a constant and dynamic process depending upon several physicochemical factors, including discharge, temperature, groundwater retention time, and vegetation, etc. (Lojen et al., 2004, 2009).

Sediment formation in alternate lotic and lentic environments thus shows the dynamics of the river system. The annual tufa growth rates estimated on the laminated specimen as the thickness of couplets of laminae varied between 1 (Jaruga power plant at Skradinski buk) (Lojen et al., 2004) and 5 mm (this study, measured on the specimen taken at the overflow between Upper and Lower Brljan Lake, site K3, Figure 3.1) (Rovan et al., 2021). Precise measurements were performed in 2018 – 2019 on artificial substrates placed at 14 micro-locations within the Skradinski buk waterfall system at the head of the Krka estuary, using a macro-photogrammetry device in a contactless manner, which showed tufa growth rates between 0.3 and 19.3 mm/year (Marić et al., 2020).

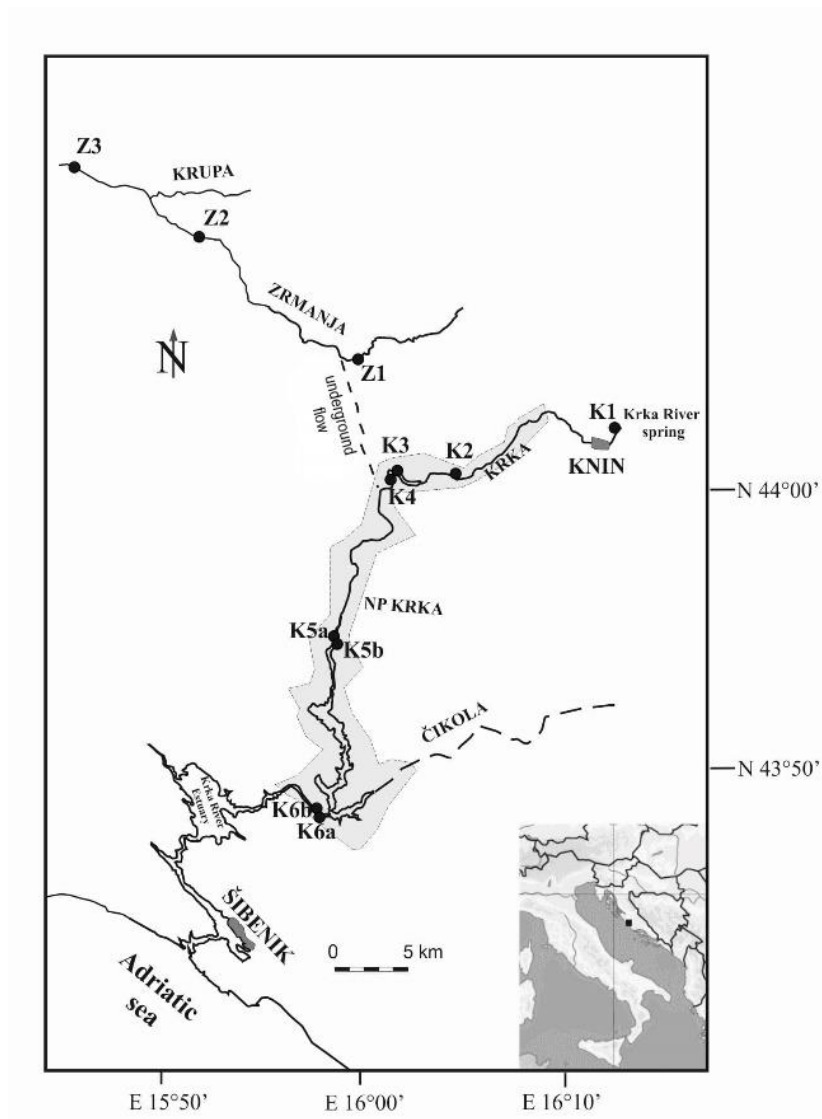


Figure 3.1: Location of the Krka river and sampling sites.

Chapter 4

Materials and Methods

The essential aspect of the success of any environmental investigation mainly depends on the collection of representative samples, sample handling without any contamination, storage and adopting adequate sample decomposition techniques if required and eventually accurate and precise estimation of parameters of interest by standard or advanced analytical techniques (Das, 2008). In this section, sampling, elemental analysis, concentration, and isotopic analysis are described.

For the present study, river water and tufa deposit samples were already collected in September 2019. Water samples were analyzed to determine the content of major ions (Ca^{2+} , Mg^{2+} , Na^+ , K^+ , Sr^{2+} , Ba^{2+}), dissolved inorganic carbon (DIC), total alkalinity and isotopic analysis. Tufa, bedrock and soil samples were analyzed for mineralogical, elemental and isotopic composition.

4.1 Sampling Scheme and Procedures

The samples were collected from 9 different sites shown in Figure 3.1. Primary samples sites' locations are shown in Table 4.1.

Table 4.1: Coordination locations, elevations and their distance from the spring.

Sampling points	Coordinate N	Coordinate E	Elevation (m)	Distance from the spring (km)
Spring (K1)	44°02'30''	16°14'05.60''	224	0
Bilušića buk (K2)	44°00'47.39''	16°04'06.35''	205	16
Brljan lake (K3)	44°00'33.63''	16°02'37.04''	186	18.8
Manojlovac (K4)	44°00'54.95''	16°01'35.94''	150	20.5
Roški slap Ogrlice (K5a)	43°54'30.02''	15°58'39.20''	72	35
Roški slap pod ogrlicami (K5b)	43°54'30.02''	15°58'39.20''	70	35.5
Skradinski buk (“Nevenov slap”) (K6a)	43°48'13.04''	15°57'54.19''	34	49

Skradinski buk (“Glavni slap”) (K6b)	43°48'13.04"	15°57'54.19"	32	49.5
Zrmanja Mokro polje (Z1)	44°05'31.65"	16°02'01.18"	196	16
Zrmanja Kaštel Žegarski (Z2)	44°09'43.09"	15°51'27.98"	55	38
Zrmanja Berberov buk (Z3)	44°11'46.87'	15°46'10.56"	19	50

The water samples were collected from the channel centre or from where the water was easy to access, but nevertheless most well mixed. If access was not easy, the samples were taken from the stream bank. Samples were collected using a high-density polyethylene (HDPE) jug attached to a rope rolled up to a wide plastic holder. Before taking the samples, the jug was rinsed three times, and extreme caution had been taken to keep the sampling and measuring equipment clean and maintain it in good working condition before and after the use.

The water pH and temperature (T), redox potential and conductivity were measured using the Ultrameter II 6 PFC (Myron Company). The total alkalinity of the river water was determined by Gran titration (Gieskes, 1974) in approx. 50 mL samples using 0.05 M HCl (Sigma Aldrich) with a precision of $\pm 1\%$ within 8 h after sample collection. Samples for alkalinity were filtered through 0.20- μm filter Sartorius (Minisart 16534 K). The water samples were stored in precleaned high-density polyethylene (HDPE) containers. Samples for the metal analyses were filtered on-site, too, through 0.45- μm pore size filters (Minisart 16555K) and acidified with concentrated supra-pure HNO_3 (Merck). Major element concentrations (Ca, Mg, Sr, K and Na) were determined using an Agilent 7900x ICP-MS (Agilent Technologies, Tokyo, Japan). All water samples were stored in the refrigerator at 4°C until analysis. Single standard solutions with 1000 mg/L (Merck) concentration were used.

4.1.1 Tufa bedrock and soil sampling

Nine recent tufa samples and twelve old tufa samples were collected. Characteristics of sampling locations were the same as for water samples. After the collection, they were placed in accurately marked plastic bags. In the laboratory, they were dried at 60°C temperature, crushed to powder and stored in new plastic bags. The crushed samples were then analysed for elemental, mineralogical and isotopic compositions. Additionally, 7 bedrock and 8 soil samples were also taken.

4.2 Isotopic Composition of Dissolved Inorganic Carbon

The isotope composition of dissolved inorganic carbon (DIC) was measured using a method by Miyajima et al., (1995); Spötl, (2005). The septum vials having a volume of 3.7 mL and 100-200 μL of phosphoric acid were tightly closed and purged for 2 minutes with 50 mL/min He (6.0). The He flushed septum vials were injected with a 1 mL sample, and the headspace CO_2 was analysed with IsoPime 100 isotope ratio mass spectrometer (IRMS) with MultiflowBio preparation module. As working standards, a standard solution of Na_2CO_3 with a known $\delta^{13}\text{C}$ values of $-10.8 \pm 0.2 \text{‰}$ and $-4.2 \pm 0.2 \text{‰}$ were used. Measurements were calibrated with CO_2 evolved from NBS18 and NBS19 certified reference materials ($\delta^{13}\text{C}$ values is 1.95 ‰ VPDB) in reaction with 100 % phosphoric acid after 24h at 25°C.

4.3 Isotopic Compositions of Hydrogen ($\delta^2\text{H}$) and Oxygen ($\delta^{18}\text{O}$) of Water

The isotopic analysis of hydrogen ($\delta^2\text{H}$) and oxygen ($\delta^{18}\text{O}$) of water were performed according to the modified IAEA Technical procedure note no. 43 (Tanweer et al., 2009), using the $\text{H}_2\text{-H}_2\text{O}$ (Coplen et al., 1991) and $\text{CO}_2\text{-H}_2\text{O}$ (Avak & Brand, 1995; Epstein & Mayeda, 1953) equilibration techniques. Measurements were performed with dual-inlet isotope ratio mass spectrometer Delta Plus (Finnigan MAT GmbH, Bremen, Germany) with a custom-built automated $\text{H}_2\text{-H}_2\text{O}$ and $\text{CO}_2\text{-H}_2\text{O}$ equilibrator HDOeq 48 Equilibration Unit (M. Jaklitsch).

4.4 Chemical Analyses

Chemical analyses of water consist of total alkalinity and major and trace element ion concentrations measurements (Ca^{2+} , Mg^{2+} , Sr^{2+} , etc.), and stable isotope analyses of carbon, oxygen, hydrogen, and Sr. The analyses of tufa and carbonate rock samples include elemental composition and stable isotope analyses of carbon, oxygen, and Sr. Their analytical methods are described as follows.

4.4.1 X-Ray diffraction analyses

All visible plant and bedrock pebbles remains were removed, and samples were pulverized in a vibrating disk mill. The phase composition of the tufa samples was determined using the X-ray diffraction method (XRD) using an Empyrean X-ray diffractometer manufactured by PANalytical (The Netherlands), equipped with a micro diffraction modulus. The analyses and data treatment were performed at the Slovenian National Building and Civil Engineering Institute.

4.4.2 X-Ray fluorescence analysis

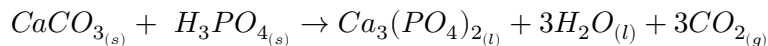
Elemental analyses of the bedrock and tufa samples were performed using X-ray fluorescence spectroscopy (Thermo Scientific ARL PERFORM'X WD XRF spectrometer) for materials and minerals analysis with OXAS software at the Slovenian National Building and Civil Engineering Institute. A mixture of Fluxana powder (FX-X50, 50% Lithotetraborate and 50% Lithometaborate) in sample: Fluxana ratio of 1:10 was prepared for melted disks. A small amount of LiBr was added to prevent glueing of the melt onto the platinum vessel. The temperature of the ignition was 950°C . The analytical errors were calculated $< 0.1\%$ for Sr and Ca, $< 6\%$ for Mg, Al, and Si, and $< 15\%$ for Na and K.

4.4.3 Analyses of sedimentary organic carbon

Analysis of sedimentary organic carbon (C_{org}) was performed. Approximately 7 mg of sample was weighted into the silver capsules (9×5 mm) for each sample. The samples were gradually acidified with 0.05M, 0.1M, 0.5M, 1M, 2M and 6M HCl. When no carbonate dissolution occurred after acidification with 6M HCl, samples are ready to analyze (Pella & Colombo, 1978). Then, these capsules were dried using an oven at 60°C overnight and subsequently tightly closed and analyzed using the Europa Scientific 20-20 isotope ratio mass spectrometer at the Department of Environmental Sciences, Jožef Stefan Institute, Ljubljana. Sorghum wheat and USGS40 are used as reference material.

4.5 Stable Isotope Analyses of Bedrock and Tufa

The method used for the analyses of stable carbon and oxygen isotopic composition of carbonates is based on the treatment of carbonate samples with orthophosphoric acid (McCrea, 1950) to extract carbon in the form of CO_2 .



The phosphoric acid which was used for the analysis was prepared by heating 85 % H_3PO_4 (Acros Organics, UK) and 99.9 % P_2O_5 (Sigma Aldrich, UK) following the procedure described in Sharp (2007) and this solution is known as 100 % orthophosphoric acid with density $\sim 1.9 \text{ g/cm}^3$ since it does not contain any water.

About 10 mg samples were weighed in Labco Exetainers® vials, dried overnight at 60°C and flushed with He (6.0). 0.3 mL of H_3PO_4 were injected into each vial with extreme caution. Samples were digested for 72 h at 40°C in a thermoblock fitted to the ANCA TG preparation unit for trace gas analysis of the Europa Scientific 20-20 isotope ratio mass spectrometer. All samples were measured in triplicate, and the results were accepted if the standard deviation was equal or less than 0.1 ‰ for both $\delta^{13}\text{C}$ and $\delta^{18}\text{O}$. If the deviation was larger, the analysis was repeated until the required precision was achieved. The stable isotope analysis of carbon $\delta^{13}\text{C}_{\text{carb}}$ was analysed on Europa Scientific 20-20 isotope ratio mass spectrometer upgraded with a Sercon HS source assembly and 20-22 electronic suite (Sercon Ltd., Crewe, U.K) in the same way. Calibration of measurements was performed by VPBD scale using NBS 19 (Limestone, NIST) and IAEA CO-9 (Barium carbonate) certified references materials.

4.6 Sr Isotope Analyses

For the determination of Sr isotopes, all chemical procedures and measurements were completed under clean room conditions. Analytical reagents were prepared with clean laboratory equipment soaked overnight in 10% HNO_3 and washed with deionized water (18.2 MΩ cm, Millipore Milli-Q-Plus). The Sr extraction procedure includes sample digestion, sample evaporation, resin cleaning, column preparation and Sr extraction. Their details are described below.

4.6.1 Sample digestion for bulk samples

100 mg of each sample (tufa and rock) were weighted in the 30 mL vials. 10 mL of concentrated HNO_3 was added to the samples and kept for 24 hours at room temperature. Then, the samples were centrifuged twice at 4000 rpm for 10 minutes and stored in the refrigerator and separated the extraction solution from the solids. Sr concentration in the extracts was determined by an inductively coupled plasma mass spectrometer (ICP-MS)(7700x, Agilent Technology, Tokyo, Japan).

4.6.2 Sample preparation for carbonate leaching

The carbonate leaching from the samples was performed as described in detail by Rován et al., (2020). An aliquot of 100 mg of each sample (tufa, bedrocks, and soil) was weighed in vials. To extract the carbonate-bound Sr, a solution of 1 M sodium acetate (NaAc) and 25 % acetic acid (Hac) was prepared. In the next step, 10 mL of the prepared solution was added to the solid samples. Dissolution was performed first by shaking them for 2 hours at room temperature at 2.75 mot/min and then centrifuging at 4000 rpm for 20 minutes. All

the samples were filtered through 0.2- μm membrane filters (Sartorius Minisart 16534K) and washed twice with 5 mL Milli-Q water after reperforming the centrifugation. Sr concentration in the extracts was determined by ICP-MS.

4.6.3 Sample evaporation

Volume containing 50 μg Sr of each sample was transferred into a Teflon vial and put on a sand bath for evaporation at 90°C. After evaporation, 1 mL of concentrated HNO_3 and 1 mL of hydrogen peroxide (H_2O_2) were added to the remaining solid in order to additionally destroy the organic matter. The solution was left to evaporate until dry and was then re-dissolved in 1mL 8M HNO_3 .

4.6.4 Sr extraction

Sr resin Eichrom® (SR-B50-S Triskem International, France) (100-150 μm) was chosen for matrix elements (i.e., Rb) removal. Acid cleaned columns were loaded with 0.3 g of Sr resin. The resin was then washed with 3 mL Milli-Q water, 1 mL 6M HCL, 10 mL Milli-Q water in sequence and conditioned with 3 mL 8M HNO_3 , 10 mL Milli-Q water and 3 mL 8M HNO_3 to the columns. The sample solution was loaded onto the columns, and Rb was removed with 5 mL of 8M HNO_3 . The Sr fraction was eluted and collected in vials with 10 mL Milli-Q water. Sr isotope ratios were measured using multi collector ICP-MS (II, Nu Instruments Ltd, Ametek Inc., Wrexham, UK).

4.7 Thermodynamics Modelling and Calculations

Geochemical calculations were performed with the PHREEQC computer program (Parkhurst & Appelo, 1999) by using the PhreeqC database in order to calculate dissolved inorganic carbon, carbon species concentration, saturation indices with respect to calcite and partial pressure of CO_2 ($p\text{CO}_2$) in the water samples.

The $p\text{CO}_2$ was obtained from the equation below:

$$p\text{CO}_2 = \frac{[\text{HCO}_3^-][\text{H}^+]}{K_{\text{H}}K_1}$$

where K_{H} and K_1 are the temperature-dependent Henry's law and first association constant for CO_2 in water.

$$\text{SI}_{\text{calcite}} = \log \left(\frac{[\text{Ca}^{2+}][\text{CO}_3^{2-}]}{K_{\text{calcite}}} \right)$$

where K_{calcite} is the solubility product of calcite (Appelo & Postma, 2009), and activities are shown by brackets. The Ca^{2+} concentration in equilibrium with calcite was also calculated with the same program.

4.8 Calcite Precipitation Rate

The precipitation rate of calcite in the carbonate-dominated water can be calculated by knowing Ca^{2+} concentration, water temperature and hydrodynamics conditions (Dreybrodt, 1988), and precipitation rate can be approximated by the Diffuse Boundary

Layer (DBL) model under turbulent flow, developed by (Buhmann & Dreybrodt, 1985) and (Dreybrodt et al., 1992). For an $\text{H}_2\text{O}-\text{CO}_2-\text{CaCO}_3$ system supersaturated with respect to calcite, the precipitation rate of CaCO_3 (R_{calcite}) can be calculated from:

$$R_{\text{calcite}} = \rho \cdot (C - C_{\text{eq}})$$

Where ρ is a reaction rate constant, C is the actual concentration of Ca^{2+} ions in the water, and C_{eq} is the equilibrium Ca^{2+} concentration with respect to calcite and pCO_2 in the water. The calculations of precipitation rate take into account the existence of a diffusion boundary layer (DBL) developed by (Dreybrodt & Buhmann, 1991). The model assumes DBL of thickness φ that separated the calcite surface from the turbulent bulk of thickness ω . The DBL factor included in the reaction constant ρ depends on temperature, the pCO_2 in the solution, on the thickness of the DBL (φ), and because of the slow conversion of HCO_3^- into CO_2 , also on the thickness of the water layer above the surface (ω) to which calcite is precipitated (Bono et al., 2001).

The calcite precipitation rate in the Krka river was calculated for tufa samples from sampling sites K2-K6b. The DBL thickness (φ) was set to 100 μm . The thickness of the water layer above the precipitated calcite surface (ω) was set to 10 cm. The ρ values were experimentally determined by (Liu & Dreybrodt, 1997) and were considered in our calculations based on measured water temperature at constant pCO_2 (10^{-3} atm). The precipitation rate of calcite formation in the Krka river was calculated using a method thoroughly explained by (Zavadlav et al., 2017).

Chapter 5

Results

5.1 Physicochemical Characteristics

The water temperature had an increasing trend downstream of the spring (Figure 5.1a). The river water temperature ranged from 9.90 °C at the spring to 23.60 °C at K6b. The pH value in the stream water varied from 7.11 to 8.31 (average 8.02 ± 0.35 ; where \pm applies to 1σ) (Figure 5.1b). In general, the pH was the lowest at spring, the and there was a significant increase in the pH value at K2, 16 km downstream, while further, it fluctuated between 8.07 and 8.15. At the same temperature, pH varies in a range of values. Overall, it had an upward trend downstream of the river.

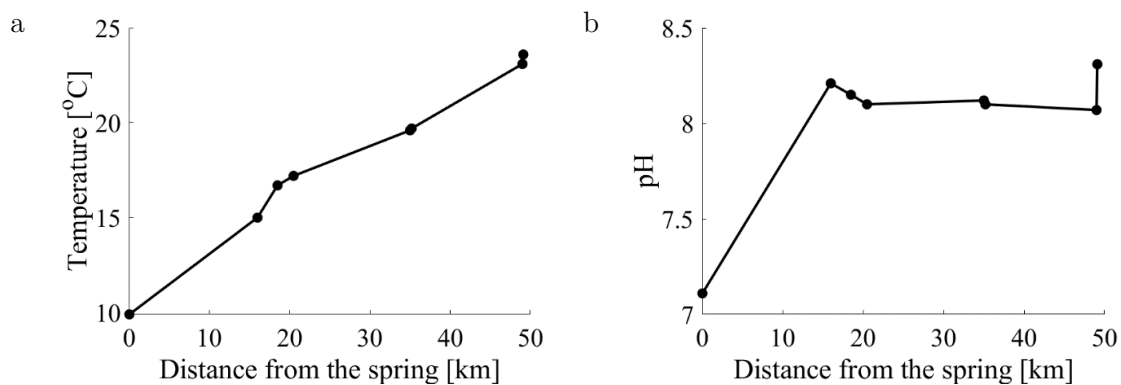


Figure 5.1: Downstream variation of (a) temperature and (b) pH.

In electrical conductivity, there was an increase between the site K1 ($426 \mu\text{S cm}^{-1}$) and the first tufa barrier K2 ($726 \mu\text{S cm}^{-1}$) and then it gradually decreased downstream to the value $469 \mu\text{S cm}^{-1}$ at the lowermost waterfall K6 (Figure 5.2a). The Eh value of the river decreased between the site K1 to K3, 18.8 km downstream from 111 mV to 94 mV. Then there was an increase, but at K5 and K6, considerable differences in Eh were observed between both riverbanks (Figure 5.2b).

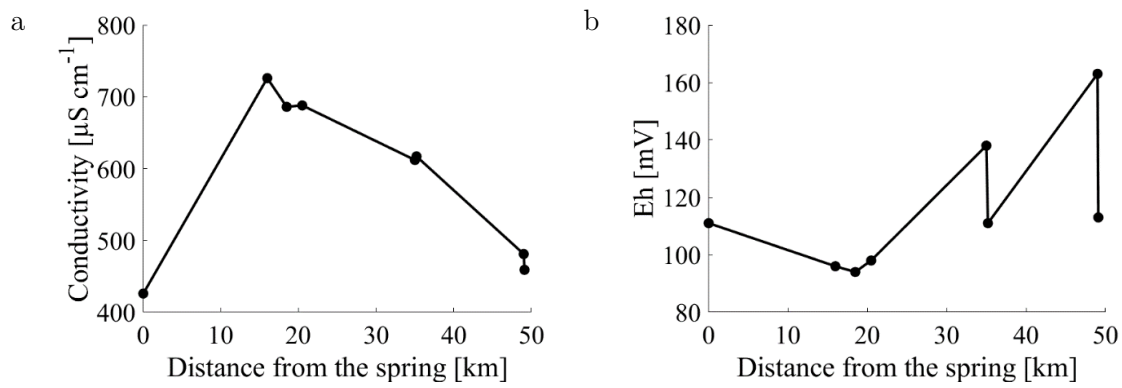


Figure 5.2: Downstream variation of (a) conductivity and (b) Eh in the Krka river water.

5.1.1 Cations and DIC

Dissolved major cations had the lowest concentration at the K1 site and the highest at sites K2-K4, as shown in Figure 5.3a,b,c,d. Further on, they gradually decreased.

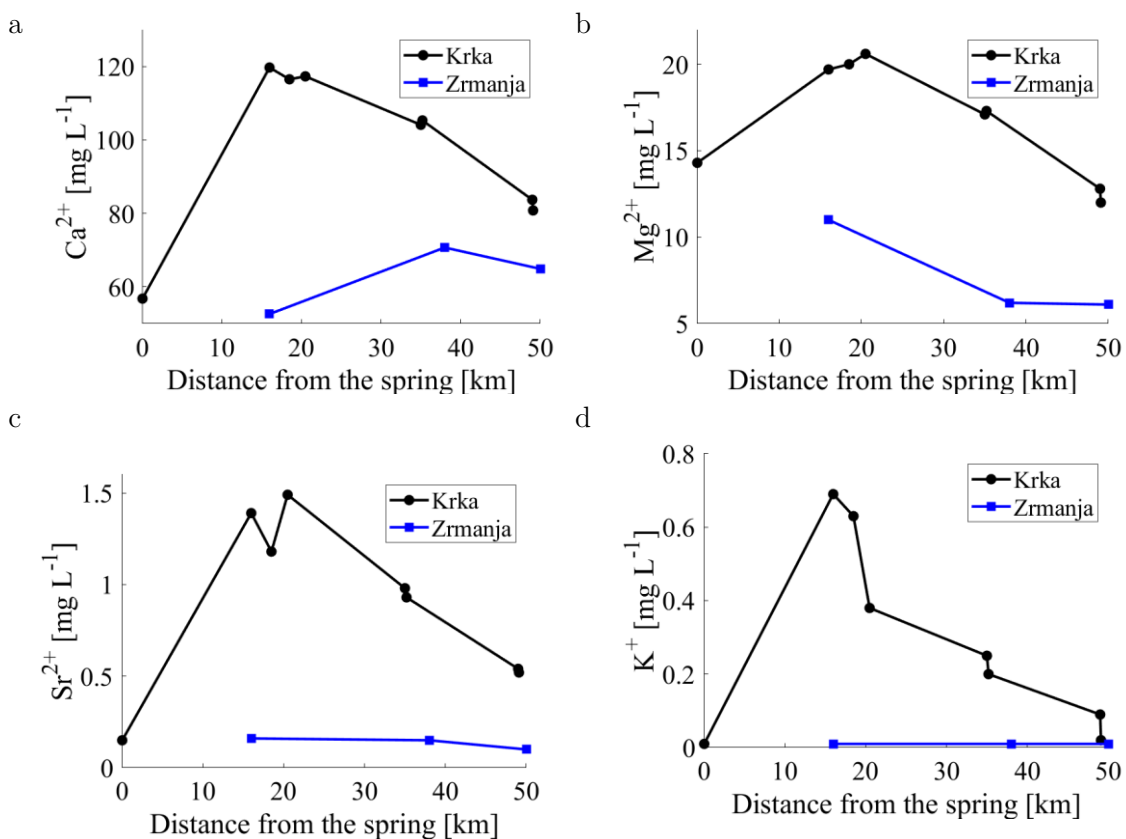


Figure 5.3: Downstream variation of (a) Ca^{2+} , (b) Mg^{2+} , (c) Sr^{2+} and (d) K^{+} content in the Krka river.

All the cations were lower in the Zrmanja river, which is evident from Figure 5.3a,b,c,d.

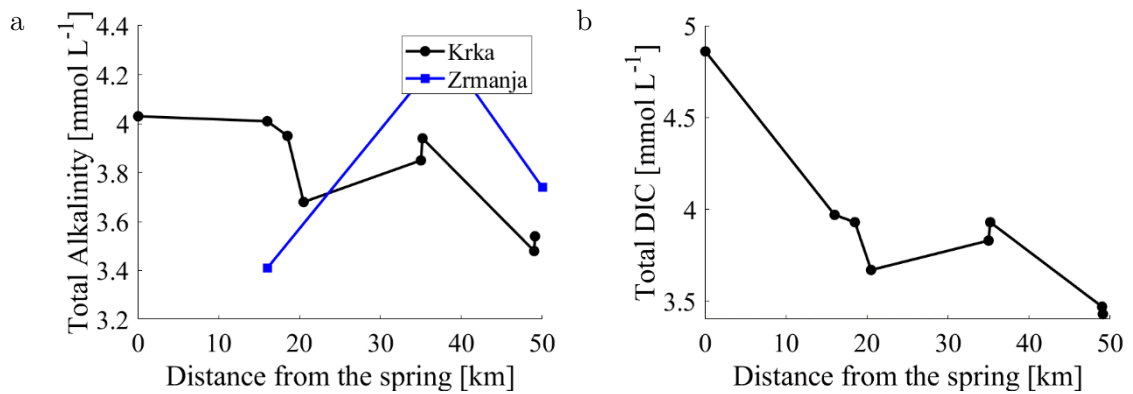


Figure 5.4: (a) Total alkalinity and (b) total DIC concentration downstream variation in the Krka river.

The total alkalinity in the Krka river showed a decreasing trend downstream the river (Figure 5.4a). The alkalinity ranged from 3.48 to 4.03 mM, and the highest value was measured at site K1 and lowest at K6. The alkalinity ranged from 3.41 to 4.30 mM in the Zrmanja river. The total dissolved inorganic carbon (DIC) (Figure 5.4b) in the Krka river water ranged from 3.43 to 4.86 mmol/L, with the highest value at the spring and the lowest at the lowermost sampling site K6. The most abundant carbon species in the Krka waters was the HCO_3^- ion, accounting for 81 % in the spring and 93 to 95 % in the stream water.

5.2 Elemental Ratios

The Mg/Ca and Sr/Ca molar ratios of the Krka and Zrmanja water had been calculated. The Mg/Ca ratio ranged from 0.25 to 0.42 (Figure 5.5a). The highest ratio was observed at site K1 and the lowest at the lowermost waterfall, K6. It decreased between K1 and the first waterfall K2 from 0.42 to 0.27, while afterwards, the ratio varied between 0.25 to 0.29, whereas in the Zrmanja water, the Mg/Ca ranged from 0.15 to 0.35.

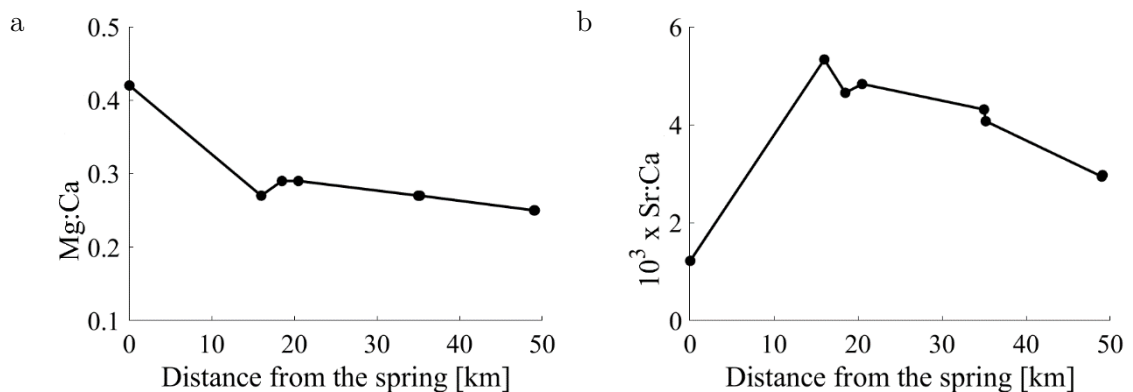


Figure 5.5: Variation of (a) Mg:Ca and (b) $1000 \times \text{Sr:Ca}$ molar ratios downstream the spring in the Krka river.

In contrast to the Mg/Ca molar ratio, $1000 \times \text{Sr/Ca}$ had the lowest ratio at site K1 and ranged from 0.12 to 0.58 (Figure 5.5b). The highest ratio of Sr/Ca was calculated at site K4. A sudden increase from 0.12 to 0.53 had been observed between the site K1 and K2, whereas downstream of K4, a decreasing pattern was observed. In the Zrmanja river, the Sr/Ca ratio was ranging from 0.07 to 0.14.

5.3 Saturation Index (SI_{calcite}) and Partial Pressure of CO_2 ($p\text{CO}_2$)

The calculated saturation indices ranged from -0.40 to 1.05. The downstream pattern was shown in Figure 5.6a, where the lowest SI_{calcite} was calculated at K1 and the highest at the last waterfall, K6. The SI_{calcite} significantly increased between K1 and K2 from -0.40 to 1.03, and afterwards, it fluctuated between 0.83 to 1.05 downstream.

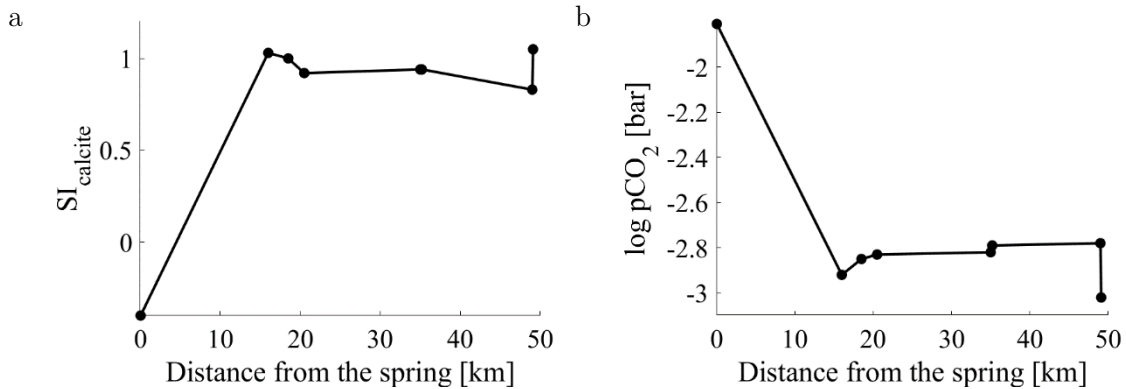


Figure 5.6: Variation of (a) SI_{calcite} and (b) $\log p\text{CO}_2$ downstream the spring in the Krka river.

On the contrary, the calculated $p\text{CO}_2$ was the highest at K1 and the lowest at K6 (Figure 5.6b). A significant decrease was observed in $p\text{CO}_2$ between the site K1 and K2, but it remained above the equilibrium with the atmosphere on the entire course of the river. SI_{calcite} downstream pattern was a mirror image of the $p\text{CO}_2$.

5.4 Stable Isotopes

5.4.1 Isotopic composition of river water

The $\delta^{18}\text{O}$ values of the Krka river water ranged from -8.92 ‰ to -7.50 ‰ with the average value -8.26 ± 0.48 ‰. The downstream plot is shown in Figure 5.7. The lowest $\delta^{18}\text{O}$ value was observed at site K1 and the highest at site K6.

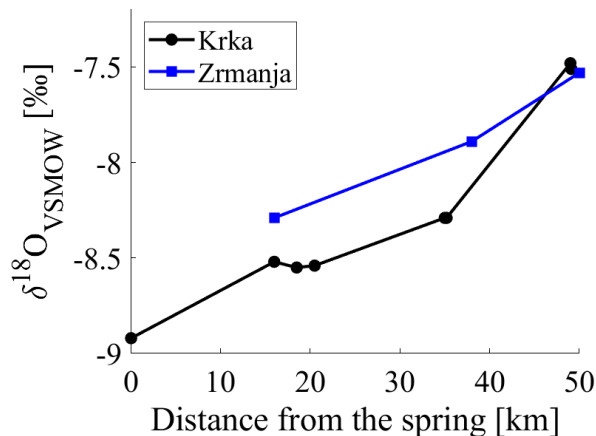


Figure 5.7: Downstream pattern of $\delta^{18}\text{O}$ in the Krka and Zrmanja river water.

It showed an increasing trend from K1 to the last waterfall, K6. The $\delta^{18}\text{O}$ value ranged from -8.29‰ to -7.53‰ in the Zrmanja river.

5.4.2 Isotopic composition of dissolved inorganic carbon (DIC) ($\delta^{13}\text{C}_{\text{DIC}}$)

The $\delta^{13}\text{C}$ values of DIC ($\delta^{13}\text{C}_{\text{DIC}}$) in the Krka waters ranged from -11.40‰ to -8.01‰ (average -9.34‰) (Figure 5.8).

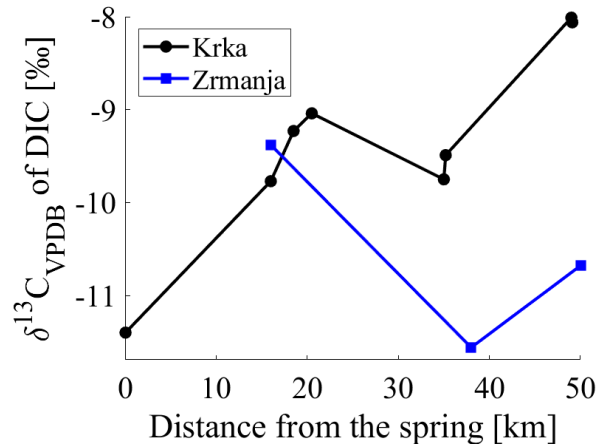


Figure 5.8: $\delta^{13}\text{C}$ variation in downstream of the spring of the Krka and Zrmanja rivers.

The highest $\delta^{13}\text{C}$ value was observed at K6 and the lowest at K1. The $\delta^{13}\text{C}$ value generally increases downstream. The downstream profile of isotopic composition of DIC $\delta^{13}\text{C}$ was the mirror-image of the DIC concentration plot (Figure 5.4b). In the Zrmanja river, the $\delta^{13}\text{C}$ value ranges from -11.56‰ to -9.38‰ .

5.4.3 Isotopic composition of Sr in water

The $\delta^{88}\text{Sr}$ value in river water (Figure 5.9) increased between K1 (0.09‰) and K2 (0.25‰), while further downstream, the $\delta^{88}\text{Sr}$ values varied between 0.08 and 0.19‰ . The lowest $\delta^{88}\text{Sr}$ value was analysed at K5b.

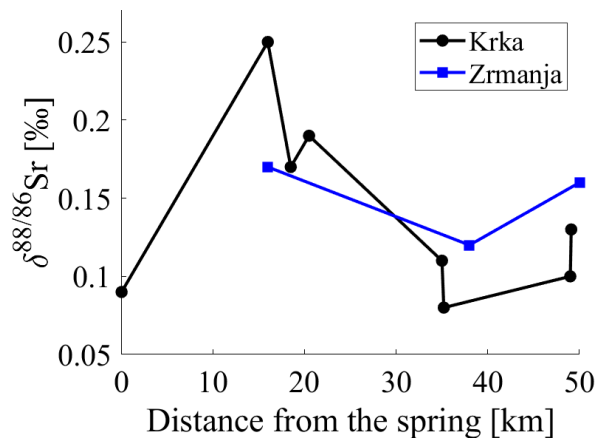


Figure 5.9: Downstream variation of $\delta^{88/86}\text{Sr}$ in the Krka and Zrmanja rivers.

In the Zrmanja river, the $\delta^{88}\text{Sr}$ value of dissolved Sr decreased from 0.17 (at Z1) to 0.12 ‰ (at Z2) and the $\delta^{88}\text{Sr}$ value again increased to 0.16 ‰ at the lowermost sampling site Z3.

5.5 Tufa

The results of geochemical and isotopic analysis of tufa are listed in Table 5.2.

5.5.1 Non-carbonate fraction

The non-carbonate mineral fraction was approximated as the sum of Al_2O_3 , SiO_2 , Fe_2O_3 , Na_2O and K_2O measured with XRF analysis. The non-carbonate fraction in tufa ranged from 1.52 to 8.63 wt. % and has a decreasing pattern downstream the river (Figure 5.10) with some fluctuations at the site K5, where the non-carbonate amount was similar to that at K3. The amount of the non-carbonate fraction of the site Z3 (5.24 wt. %) was in the range of the values of the Krka river. Moreover, the bulk Mg/Ca ratio in tufa decreased downstream from 0.07 to 0.03 (Table 5.2) and strongly correlated with the non-carbonate amount ($r^2 = 0.85$).

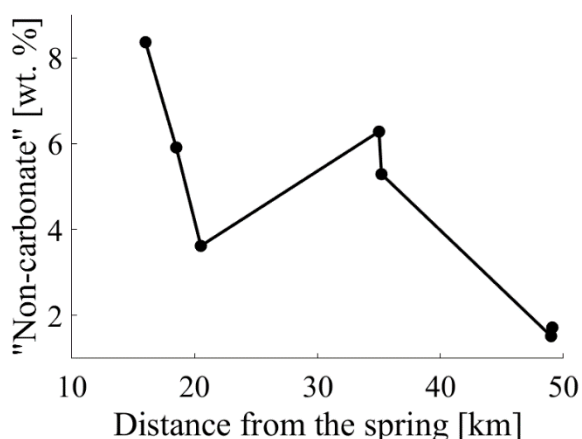


Figure 5.10: Downstream variation of non-carbonate fraction in tufa.

The Mg/Ca ratio in tufa from the Zrmanja river (Table 5.2) was also in the same range of values as in the Krka river (0.05). The leached carbonate fraction Mg/Ca ratio was below 0.01 at all sites. The carbonate-bound Mg fraction was low at all sites (11 to 23 %) in contrast to the Ca, which is 80 to virtually 100 % to the carbonate fraction. The fraction of carbonate-bound Mg was in strong negative correlation with the non-carbonate in tufa ($r^2 = -0.88$). The Sr/Ca was not found correlated with the non-carbonate fraction (Table 5.2).

5.5.2 Sedimentary organic carbon (SOC)

The sedimentary organic carbon (SOC) concentration in recent tufa ranged from 0.27 to 1.14 wt. % with the average 0.62 ± 0.27 wt. %. There was no clear trend (Figure 5.11) in the concentration of SOC in tufa. The isotopic composition of organic carbon ($\delta^{13}\text{C}_{\text{org}}$) ranged from -34.74 to -28.57 ‰ (average -31.57 ± 2.32 ‰). No clear downstream trend was observed. The C/N elemental ratio in recent tufa ranged from 9.8 to 22.5.

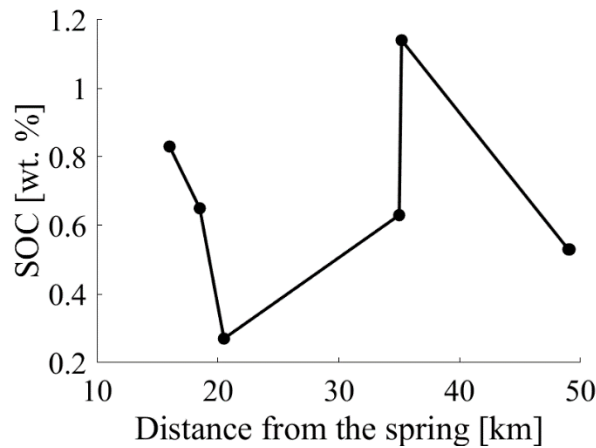


Figure 5.11: Spatial variability pattern of SOC concentration in tufa.

5.5.3 Stable isotope composition of carbon and oxygen

The carbon and oxygen isotopic composition of recent tufa precipitated in the Krka river showed relatively narrow variability with $\delta^{13}\text{C}_{\text{Tufa}}$ and $\delta^{18}\text{O}_{\text{Tufa}}$ ranged from -10.34‰ to -8.72‰ (average $-9.51 \pm 0.59\text{‰}$) and -8.63‰ to -7.19‰ (average $-7.98 \pm 0.44\text{‰}$), respectively. The downstream pattern is shown in Figure 5.12. The only tufa sample from the Zrmanja river had the $\delta^{13}\text{C}_{\text{Tufa}}$ value similar to the lowermost waterfall K6 of the Krka river (-10.31‰), while the $\delta^{18}\text{O}_{\text{Tufa}}$ value was -7.47‰ .

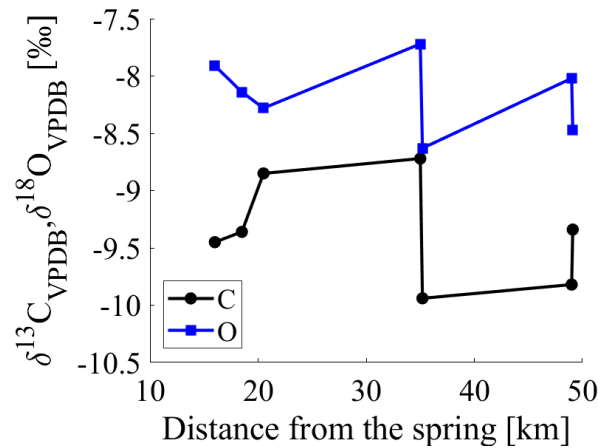


Figure 5.12: Downstream variations in $\delta^{18}\text{O}$ and $\delta^{13}\text{C}$ values in tufa.

5.5.4 Stable and radiogenic isotope of Strontium

The radiogenic and stable Sr isotopic composition in recent tufa ($^{87}\text{Sr}/^{86}\text{Sr}$ and $\delta^{88}\text{Sr}_{\text{Tufa}}$, respectively) ranged from 0.70750 to 0.70762 (average 0.70757 ± 0.0001) (Figure 5.13a) and 0.00‰ to 0.20‰ (average $0.03 \pm 0.25\text{‰}$) (Figure 5.13b), respectively.

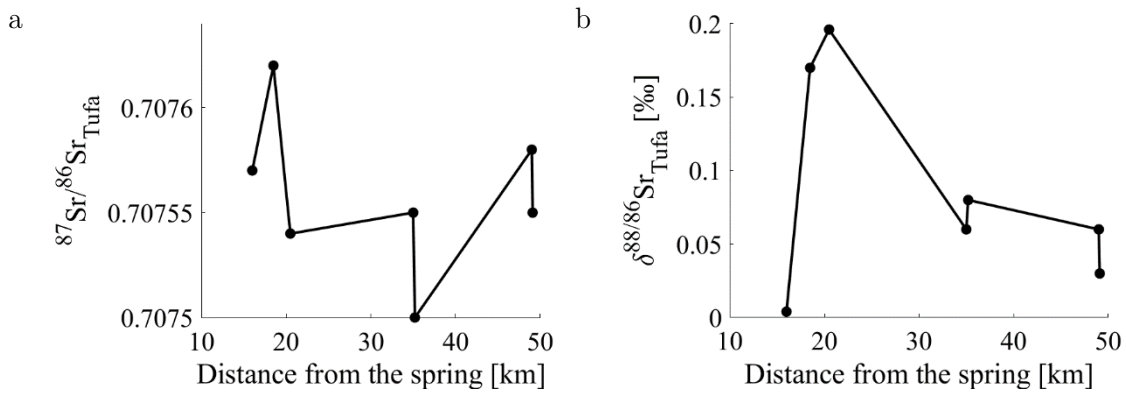


Figure 5.13: Downstream variability in a) $^{87}\text{Sr}/^{86}\text{Sr}$ and b) $\delta^{88/86}\text{Sr}$ in tufa.

The only tufa sample from the Zrmanja river had the $^{87}\text{Sr}/^{86}\text{Sr}$ value higher than any site of the Krka river (0.70781), whereas the $\delta^{88}\text{Sr}_{\text{Tufa}}$ value is in the range of values at the lower part of the Krka river (-0.23 ‰). The value of leachable $\delta^{88}\text{Sr}$ ranged from 0.00 ‰ to 0.10 ‰ in recent tufa.

5.6 Bedrock and Soil

The results of geochemical and isotopic analysis of bedrock and soil are listed in Table 5.2. Most of the samples collected from the K2, K3 and K4 sites were limestone or carbonate-rich clastic rocks (marl and breccia at K4, conglomerate at K5b) with non-carbonate fraction between 2 and 4.2 wt. %, except at the Krka river spring sampling site, the sandstone had a non-carbonate fraction of 45%.

5.6.1 Stable isotope composition of C and O

The C and O stable isotope composition ranged from -9.48 ‰ to -2.18 ‰ and -9.21‰ to -5.91 ‰, respectively, in soil, whereas these values ranged from -2.26 ‰ to 0.76 ‰ and -6.07 ‰ to -3.89 ‰, respectively, in bedrock samples.

$\delta^{13}\text{C}$ vs. $\delta^{18}\text{O}$ of Bedrock, soil and tufa are plotted in Figure 5.14. Two separate groups of bedrock and tufa were found.

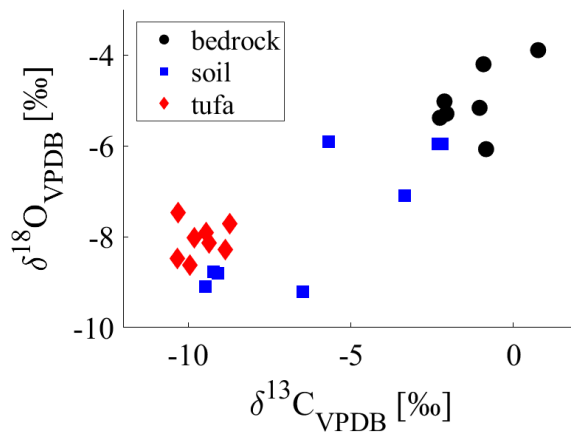


Figure 5.14: $\delta^{18}\text{O}$ and $\delta^{13}\text{C}$ in soil, bedrock and tufa.

Bedrock was enriched in heavy C and O isotopes while the soil samples lied in between these two groups, with the values ranging from typical for marine carbonate to typical of tufa. It is important to note that the lowest measured $\delta^{18}\text{O}$ value in soil (-9.48‰) was lower than in any of the tufa samples.

The average $\delta^{13}\text{C}$ values of sedimentary organic carbon in the soil ($-28.96 \pm 1.57\text{‰}$) were lower than in the bedrock ($-25.28 \pm 0.90\text{‰}$). The average Corg: N ratios in soil were about 16.3, slightly higher than the tufa (average 14.2), while N concentration was not determined in the bedrock. The $\delta^{13}\text{C}$ values Organic C of tufa plotted in between or below the soil and bedrock samples.

5.6.2 Sr in soil and bedrock

Soil and bedrock samples showed significantly lower Sr concentrations compared to the tufa samples. The Sr concentration ranged from 0.022 to 0.418 mg/g (average 0.220 ± 1.34 mg/g) in soil and 0.044 to 0.241 mg/g (average 0.138 ± 0.064 mg/g), where the bedrock samples from sites K1 and K2 contained 0.044 and 0.056 mg/g Sr, respectively, and the rest of bedrock samples contained 0.142 to 0.241 mg/g. It can be observed from Figure 5.15 that the $\delta^{88}\text{Sr}$ values are higher in soil and bedrock than in tufa.

The $\delta^{88}\text{Sr}$ values of bulk samples varied from 0.10 to 0.37 ‰ in bedrock samples and 0.19 to 0.42 ‰ in the soil, whereas the $\delta^{88}\text{Sr}$ values in leachable fraction ranged from 0.15 to 0.28 ‰ in bedrock and 0.00 to 0.16 ‰ in the soil. In the bedrock and soil samples, the Sr radiogenic isotopic ratio varies from 0.70730 to 0.70765 and 0.707659 to 0.707676, respectively. The $\delta^{88}\text{Sr}$ value in bulk samples is higher than in the leachable fraction, and in the case of $^{87}\text{Sr}/^{86}\text{Sr}$, values in bulk are greater or equal to the values in the leach.

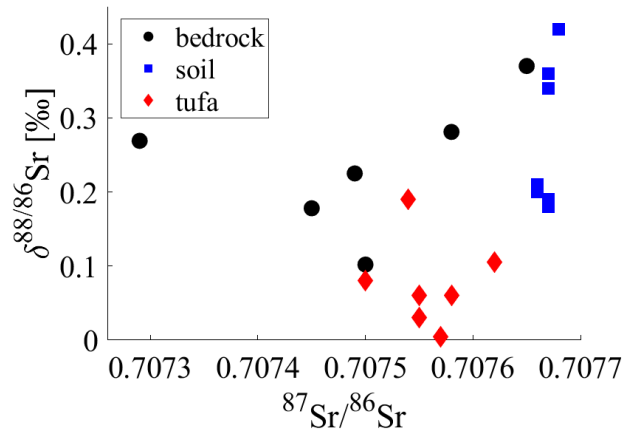


Figure 5.15: $\delta^{88}\text{Sr}$ and $^{87}\text{Sr}/^{86}\text{Sr}$ in soil, bedrock and tufa.

Table 5.1: Results of physico-chemical parameters in the Krka river and of chemical and isotopic analyses in the Krka and Zrmanja rivers.

Site	T	pH	Conductivity	Eh	Particulate matter	Total alkalinity	$\delta^{18}\text{O}$	$\delta^2\text{H}$	Conc.D IC	$\delta^{13}\text{C}$ -DIC	Ca^{2+}	Mg^{2+}	Sr^{2+}	$1000^*\text{Sr}/\text{Ca}$	Mg/Ca	pCO_2	Sicalc	R	$^{87}\text{Sr}/^{86}\text{Sr}$	$\delta^{88}\text{Sr}$
	[°C]		[$\mu\text{S cm}^{-2}$]	[mV]	[mg L ⁻¹]	[mmol L ⁻¹]	[‰]	[‰]	[mmol L ⁻¹]	[‰]		[mg L ⁻¹]		molar ratio				$10^{-9} \frac{\text{g}}{\text{cm}^2 \text{s}^{-1}}$		[‰]
K1	9.9	7.11	426	111	4.2	4.03	-8.92	-57.00	4.86	-11.40	56.8	14.3	0.15	1.22	0.42	-1.81	-0.40	NM	0.70773	0.09
K2	15.0	8.21	726	96	2.0	4.01	-8.52	-53.60	3.97	-9.77	119.7	19.7	1.39	5.33	0.27	-2.92	1.03	4.9	0.70763	0.25
K3	16.7	8.15	686	94	0.3	3.95	-8.55	-54.10	3.93	-9.23	116.5	20.0	1.18	4.65	0.29	-2.85	1.00	5.3	0.70763	0.17
K4	17.2	8.10	688	98	< 0.1	3.68	-8.54	-53.90	3.67	-9.04	117.3	20.6	1.49	5.83	0.29	-2.83	0.92	5.6	0.70769	0.19
K5a	19.6	8.12	612	138	< 0.1	3.85	-8.29	-51.80	3.83	-9.75	104.1	17.1	0.98	4.31	0.27	-2.82	0.94	5.4	0.70778	0.11
K5b	19.7	8.10	617	111	1.6	3.94	-8.29	-52.00	3.93	-9.49	105.3	17.3	0.93	4.07	0.27	-2.79	0.94	5.5	0.70773	0.08
K6a	23.1	8.07	481	163	6.5	3.48	-7.48	-47.80	3.47	-8.01	83.7	12.8	0.54	2.94	0.25	-2.78	0.83	5.2	0.70769	0.10
K6b	23.6	8.31	469	113	13.5	3.54	-7.51	-47.90	3.43	-8.06	80.8	12.0	0.52	2.97	0.25	-3.02	1.05	4.9	0.70765	0.13
Z1	NM	NM	NM	NM	1.3	3.41	-8.29	-52.50	NM	-9.38	52.6	11.0	0.16	0.35	NM	NM	NM	NM	0.70789	0.17
Z2	NM	NM	NM	NM	< 0.1	4.30	-7.89	-49.00	NM	-11.56	70.7	6.2	0.15	0.15	NM	NM	NM	NM	0.70772	0.12
Z3	NM	NM	NM	NM	0.3	3.74	-7.53	-47.20	NM	-10.68	64.9	6.1	0.10	0.16	NM	NM	NM	NM	0.70773	0.16

NM – Not Measured; K1-K6b and Z1-Z3 as mentioned in Table 4.1.

Table 5.2: Isotopic and geochemical parameters of tufa, bedrock and soil samples from the Krka river.

	Site	$\delta^{13}\text{C}_{\text{carb}}$	$\delta^{18}\text{O}_{\text{carb}}$	$\delta^{13}\text{C}_{\text{org}}$	C_{org}	non-carb	C/N	Ca	Mg	Sr	$1000 \cdot \text{Sr}/\text{Ca}$	Mg/Ca	$^{87}\text{Sr}/^{86}\text{Sr}$	$\delta^{88}\text{Sr}$	$\delta^{88}\text{Sr}_{\text{leach}}$	$\Delta^{88}\text{Sr}_{\text{t-w}}$	D_{Sr}
		[‰]	[‰]	[‰]	wt. %	wt. %			[mg g ⁻¹]		molar ratio		[‰]	[‰]	[‰]		
Tufa	K2	-9.45	-7.91	-30.11	0.83	8.36	12.9	347	13.87	0.54	0.72	0.07	0.70757	0.004	0.004	-0.24	0.13
	K3	-9.36	-8.14	-28.63	0.65	5.91	15.7	356	12.25	0.46	0.60	0.06	0.70762	0.105	0.07	-0.1	0.13
	K4	-8.85	-8.28	-28.57	0.27	3.62	22.5	370	9.63	0.53	0.65	0.04	0.70754	0.196	0.10	-0.09	0.11
	K5a	-8.72	-7.72	-33.09	0.63	6.28	14.7	357	10.91	0.35	0.46	0.05	0.70755	0.06	0.06	-0.05	0.11
	K5b	-9.94	-8.63	-34.45	1.14	5.29	9.8	356	10.94	0.48	0.62	0.05	0.70750	0.08	0.08	0.00	0.15
	K6a	-9.82	-8.02	-33.20	0.53	1.52	12.2	381	5.13	0.33	0.40	0.05	0.70758	0.06	0.06	-0.04	0.14
	K6b	-10.34	-8.47	-34.74	0.53	1.72	14.6	383	6.15	0.42	0.50	0.03	0.70755	0.03	0.03	-0.1	0.17
Bedrock	K1	-2.26	-5.38	-26.08	NM	45.17	NM	194	14.10	0.063	0.15	0.12	0.70765	0.37	0.174	--	--
	K2	-0.84	-6.07	-26.40	NM	2.04	NM	398	2.58	0.094	0.11	0.01	0.70749	0.225	0.283	--	--
	K3	-2.06	-5.29	-24.85	NM	3.92	NM	378	3.14	0.163	0.20	0.01	0.70745	0.178	0.163	--	--
	K4	-2.12	-5.02	-24.32	NM	3.98	NM	385	3.19	0.166	0.20	0.01	0.70729	0.269	0.207	--	--
	K4	0.76	-3.89	-24.11	NM	4.24	NM	377	4.23	0.205	0.25	0.02	0.70750	0.102	0.145	--	--
	K5b	-1.04	-5.16	-24.89	NM	1.97	NM	391	2.15	0.165	0.19	0.01	0.70758	0.281	0.251	--	--
Soil	K1	-2.18	-5.95	-30.21	4.03	9.21	13.9	260	74.2	0.08	0.15	0.48	0.707667	0.18	0.17	--	--
	K2	-9.48	-9.09	-30.39	8.36	10.55	16.8	348	4.58	0.418	0.55	0.02	0.70766	0.2	0.02	--	--
	K3	-6.47	-9.21	-29.31	9.19	51.98	13.7	166	18.3	0.263	0.73	0.18	0.707670	0.19	0	--	--
	K4	-9.22	-8.77	-29.23	3.47	6.71	18.0	364	3.70	0.40	0.51	0.02	0.707659	0.21	0	--	--
	K5a	-2.32	-5.95	-25.87	1.78	23.48	16.8	296	3.94	0.124	0.19	0.02	0.70768	0.42	0.05	--	--
	K5b	-5.69	-5.91	-28.90	1.93	36.10	11.9	238	10.9	0.249	0.48	0.08	0.70767	0.34	-0.01	--	--
	K6b	-9.08	-8.80	-30.71	12.8	38.63	24.4	235	8.62	0.199	0.39	0.06	0.70767	0.36	0.02	--	--

Chapter 6

Discussions

6.1 Material Sources for Tufa Precipitation

Tufa is composed predominantly of authigenic carbonate, which is exclusively formed from the solution, and detrital fraction, which originates from suspended matter in the water, sedimentary organic matter and from surface run-off (e.g. mineral and organic fraction from the soil, weathering residues of bedrock, etc.) (Arenas et al., 2014a; Capezzuoli et al., 2014).

6.1.1 Main source – river water

Rivers transport both dissolved and solid load in the suspended matter. The composition and proportions of each are governed by the water mixing, discharge, CO₂ outgassing and in-stream precipitation (Herman & Lorah, 1988; Szramek et al., 2007).

6.1.1.1 Dissolved inorganic carbon

DIC content in the river is controlled by the lithology (Telmer & Veizer, 1999; Kanduč et al., 2007a) and soil inputs from the water deriving from surface runoff, e.g. soil organic matter and soil CO₂ (Hope et al., 2004).

The concentration of DIC in the river depends on the composition of the spring water and on the processes that produce or eliminate DIC from the water, i.e. by calcite precipitation and CO₂ outgassing at the same time.

The isotopic composition of dissolved inorganic carbon is source-specific, i.e. depends upon the mixing ratio of DIC originating from carbonate bedrock dissolution and the contribution of biogenic CO₂ released into the water by the decomposition of organic matter and dissolution of soil CO₂. Typically, the $\delta^{33}\text{C}$ value of geogenic DIC at 15°C is by 2 ‰ lower than that of the bedrock (Deines et al., 1974), while the biogenic DIC deriving from soil organic matter or soil CO₂ is by 9 ‰ enriched in ¹³C compared to the CO₂ source (Mook et al., 1974). Regarding the measured $\delta^{33}\text{C}$ values of sedimentary organic carbon from soil and the river, the biogenic DIC would have the $\delta^{33}\text{C}$ value of about -18 ‰. In the present study, the $\delta^{33}\text{C}$ value of DIC at the spring (-11.4 ‰) indicates that the major fraction of DIC (about 55 ‰) derives from biogenic CO₂, which can be considered as the major source of DIC.

6.1.1.2 Metals in water

Major element ratios (Ca^{2+} and Mg^{2+}) and dissolved carbonate ions can be used for the estimation of the weathering ratio of source rock, carbonate *and* non-carbonate, which contributes dissolved load for tufa precipitation (Szramek et al., 2007, 2011). Major elements primarily derived from the dissolution of calcite, dolomite, sulphates, feldspar and clay materials, as well as from the cations exchange on clays (Hounslow, 1995). The dominant rocks in the watershed are calcite and dolomite. Their dissolution produces different Mg/Ca and $(\text{Ca}^{2+} + \text{Mg}^{2+})$ vs. HCO_3^- ratios of water.

According to the Krka river study by (Rovan et al., submitted), the dissolution of the mixture of limestone and dolomite should be close to a ratio of 1:1. However, a comparison of $\text{Ca}^{2+} + \text{Mg}^{2+}$ with DIC concentrations showed that the weathering of non-carbonates was significant. Silicates are present in the patches of clastic rocks that can be leached or carried into the aquifer and the river as suspended load with streamflow. The strong positive correlation of Mg in bedrock with non-carbonate indicates that Mg mainly occurs in silicates. The analysis of leachable Mg showed that only between 17 and 66% Mg was bound to carbonates in bedrock and 4 to 44% soil. Therefore, we conclude that the major source of dissolved Mg originates from silicate weathering while the dissolved Ca is contributed by the weathering of carbonate bedrock, which prevails in the watershed (Mamužić, 1971).

In soil, the concentration of Sr is strongly correlated to the non-carbonate fraction ($r^2 = 0.87$, Figure 6.1), while in the bedrock, no statistically significant correlation between these two parameters was observed. Therefore, we conclude that the Sr is partly derived from the non-carbonate fraction of soil and partly from the dissolution of both – carbonate and non-carbonate fractions of bedrock.

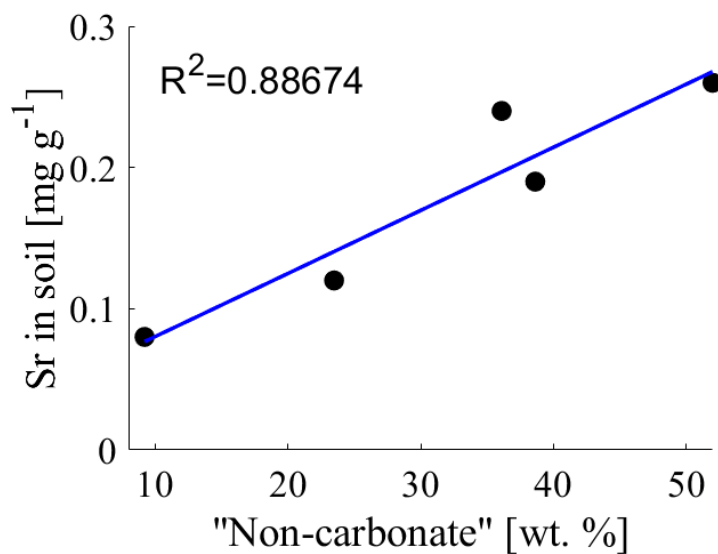


Figure 6.1: Plot of Sr versus non-carbonates in soil.

6.1.2 Detrital material

The main sources of the detrital fraction are the weathering and erosion of soil and bedrock (Fouke et al., 2000; Teboul et al., 2016). The $\delta^{13}\text{C}$ values of bedrock and soil carbonate indicated that both authigenic and detrital bedrock carbonate occur in soil. At the spring, K5a and Z3, the $\delta^{13}\text{C}$ values of soil carbonate (-2.18 ‰, -2.32 ‰, -3.34 ‰, respectively)

are typical for marine carbonates, i.e., bedrock (Colombié et al., 2011), while the soil carbonate at K2, K4 and K6b (-9.48 ‰, -9.22 ‰, -9.08 ‰, respectively), has alike or lower $\delta^{13}\text{C}$ than tufa (-10.34 to -8.72 ‰). Other soil samples had the $\delta^{13}\text{C}_{\text{carb}}$ values between the typical range of values for marine and palustrine carbonate.

Besides mineral fraction, the sedimentary organic matter can also occur in the detrital material flushed into the river with the surface runoff. The average $\text{C}_{\text{org}}:\text{N}$ ratios of sedimentary organic matter in tufa are 14.6 ± 4.3 and are similar to soil 16.1 ± 3.7 . For riverine particulate organic matter, a similar range of values was reported by Hatten et al., (2012), i.e. the $\text{C}_{\text{org}}:\text{N}$ ratio between 10 and 16 for fine particulates, 14 and 25 for coarse particulates and above 20 are typical for terrestrial organic matter derived from vascular plants (Mayer, 1998). The C:N ratio for microbial biomass is typically <10 (Kendall & Coplen, 2001). Algae have very low $\delta^{13}\text{C}$ values of -39.0 ‰ (Janssen et al., 1999) and C:N ratio of 5 to 12 (Finlay & Kendall, 2007), while mosses are characterized by $\delta^{13}\text{C}$ values -32.3 ‰ and high C:N ratio of 18 to 24 (Kanduč et al., 2007b). These low $\delta^{13}\text{C}$ values (<-30.0 ‰) of SOC in tufa show that soil organic matter and riverine organic material are present, where algae and vascular plants growing in the spray zone of the river can contribute organic carbon strongly depleted in ^{13}C (Marčenko et al., 1988).

6.2 Tufa Precipitation

The carbonates in tufa consist of two fractions authigenic, precipitated from water, and detrital, deriving from soil and bedrock. The reported element partitioning and isotope fractionations of C and O between the water and the carbonate obtained in laboratory experiments, as well as theoretical calculations, therefore, apply for authigenic carbonates only, while the presence of detrital carbonate in tufa fraction alters the bulk carbonate isotope composition and causes apparent isotope fractionation that can in some cases reach the order of magnitude of several ‰. However, only bulk carbonate C isotope composition can be measured because the detrital and authigenic carbonate cannot be separated chemically or physically before the measurements (Ortiz et al., 2009; Capezzuoli et al., 2014).

Only one water sample obtained in the late summer of 2019 was analysed for each site, while tufa precipitation is a slow continuous process that takes years to precipitate a few cm of tufa which is in fact analysed in hand samples. Therefore, the results of the calculations presented below apply only to the conditions captured during the sampling campaign and cannot be generalized.

6.2.1 C isotope variation in tufa

The $\delta^{13}\text{C}_{\text{DIC}}$ values in the Krka river water in the tufa precipitating section ranged from -9.77 ‰ to -8.01 ‰ and consistently increased downstream, while the DIC concentrations decreased, reflecting variable contributions of different carbon sources and the effects of processes in the stream that fractionate carbon isotopic composition of DIC, i.e. degassing of ^{13}C - depleted dissolved CO_2 and precipitation of carbonates.

The C Isotope fractionation between DIC and carbonate precipitates reflects environmental conditions at the time of its precipitation. To what extent tufa deposits record variance in environmental parameters mainly depends upon the processes that affect the isotopic composition of the solution and the precipitates during precipitation.

Several equilibrium equations reporting isotopic fractionation between water and calcite are available in the literature (e.g. Deines et al., 1974; Mook, 2000). However, their suitability depends on the specific situation of the studied system. The $\delta^{13}\text{C}$ value of all the

recent tufa samples measured in the current study was within the range of ± 1 ‰ deviation from the $\delta^{13}\text{C}$ values of DIC. This is in good agreement with the estimation of Romanek et al. (1992) and Jimenez-Lopez et al., (2001), with the exception at the lowermost waterfall, where samples were depleted in ^{13}C by 1.8 to 2.3 ‰ compared to the DIC of this area. However, considering the long-term data (Lojen, 2002; Lojen et al., 2004), the $\delta^{13}\text{C}$ values of both tufa samples were within the long-term range of the $\delta^{13}\text{C}$ values of DIC. Previous studies showed that in the Krka river, the carbonate precipitated close to the O isotope equilibrium only at the uppermost tufa barrier (K2). Further downstream, the discrepancy between the equilibrium $\delta^{18}\text{O}$ values of water and precipitate formed in the actual temperature range increased with an increasing annual average temperature and increasing annual temperature variability of river water (Lojen et al., 2004), which could not be explained at that time. The presence of detrital carbonate could have influenced the $\delta^{13}\text{C}$ and $\delta^{18}\text{O}$ values of tufa, which explains the large deviation from the expected results for O isotopes.

The amount of detrital and authigenic carbonate in tufa originating from soil cannot be determined since the isotopic fingerprints of soil carbonates ranged from values typical of tufa to values typical of bedrock.

6.2.2 Sr in tufa

The total dissolved concentration of Sr in river water fell within the range of 0.14 to 1.39 mg/L, which is typical for different global rivers (Galy et al., 1999; Brennan et al., 2014; Liu et al., 2017). Sr concentration showed the same downstream trend as most of the analysed cations, i.e. a significant increase between the site K1 and K2, which can be influenced both by the anthropogenic pollution (Filipović Marijić et al., 2016 unpublished; Filipović Marijić et al., 2018) and from tributaries in the Knin area (Kulušić & Borojević Šoštarić, 2014; Dedić et al., 2018). The dissolved Sr concentration decreased from the uppermost to the lowermost tufa barrier, except for the K4 site. A similar trend was also observed in the case of dissolved Mg concentration.

The decrease of Sr concentration downwards is attributed to the active self-purification processes in the river, i.e. the adsorption on mineral surfaces, sedimentation and co-precipitation with CaCO_3 (Cukrov et al., 2013). To a certain extent, Sr precipitates with CaCO_3 , however, the decreasing downstream Sr/Ca trend in the Krka river is inconsistent with abundant carbonate precipitation. This discrepancy is explained with the inflow of Sr-depleted Zrmanja river with Sr/Ca ratio lower than the Krka river (Fig. 5.3c). Obviously, the area of invasion of groundwater from the Zrmanja river occurs along the entire lower part of the Krka river flow and is not localized to the short 4 km section downstream of the Brljan Lakes, as previously reported.

The correlation observed between the temperature and the Sr/Ca molar ratio in the Krka river with ($r^2 = 0.84$, Figure 6.2) satisfies the assumption of Huang and Fairchild (2001). A very strong correlation of Sr/Ca and Mg/Ca molar ratios was found in water, which indicates that the Sr and Mg follow the same behaviour. The element partitioning also depends on many other parameters, as discussed in 1.2.3.

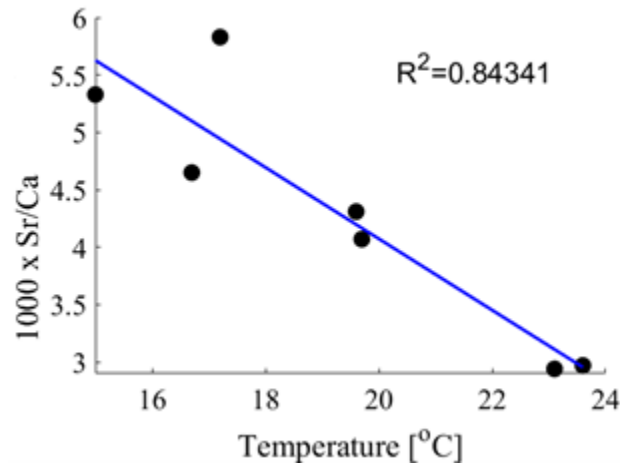


Figure 6.2: Plot of 1000 x Sr/Ca versus temperature in the Krka water.

The $\delta^{88}\text{Sr}$ value of strontium in river water varied from 0.08 to 0.25 ‰ with an average of 0.14 ‰. Sr isotopes fractionate during the dissolution of soil and bedrock as well as during the carbonate precipitation. The decreasing $\delta^{88}\text{Sr}$ values of water were inconsistent with extensive tufa formation, similar to the Sr/Ca ratios. This indicates that the invaded water from the Zrmanja river should be ^{88}Sr -depleted compared to the Krka river. However, the $\delta^{88}\text{Sr}$ values of the Zrmanja river were in the range of the Krka river. It has to be pointed out again that the results represent only the situation in September 2019, while the travel times of karst waters are on the order of magnitude of several months; therefore, no conclusions can be drawn without seasonal observations.

The distribution coefficient of Sr (D_{Sr}) for the Sr element partitioning in the tufa can be calculated as using (Huang & Fairchild, 2001):

$$D_{\text{Sr}} = (\text{Sr}/\text{Ca})_{\text{tufa}}/(\text{Sr}/\text{Ca})_{\text{water}}$$

The average calculated D_{Sr} (0.13 ± 0.02) in the current study is in the similar range of average Sr distribution coefficients, reported in the literature, 0.12-0.27 (Ihlenfeld et al., 2003; Shalev et al., 2017; Smieja-Król et al., 2017; Zavadlav et al., 2017; Ritter et al., 2018). These distribution coefficients are either mentioned in the study (Zavadlav et al., 2017; Ritter et al., 2018) or calculated from the given water and tufa geochemistry data (Ihlenfeld et al., 2003; Shalev et al., 2017; Smieja-Król et al., 2017; Ritter et al., 2018). Taking data from the previous investigations into account, Sr partitioning in the tufa is consistent for different tufa precipitation systems of the world.

Distribution coefficients of trace elements (Mg, Sr, Ba, U) are higher for tufa than for the laboratory experiments of calcite precipitation. This discrepancy indicates that there must be some other factors that are controlling the element partitioning in tufa, such as biological influence, i.e., biofilms (Rogerson et al., 2008; Saunders et al., 2014; Ritter et al., 2018) and anthropogenic activities, i.e., pollution (Lojen et al., 2009). Distribution coefficients of elements in tufa are analysed for bulk samples, which always contain some detrital fraction (usually a few wt.%), which obscures the calculated distribution coefficient. Obviously, the Sr partitioning in studied tufa deposits is also biologically and anthropogenically influenced.

Sr concentration and the $\delta^{88}\text{Sr}$ value in bulk tufa and leachable fraction were analysed. The $\delta^{88}\text{Sr}$ values in recent tufa are within the range of previously reported $\delta^{88}\text{Sr}$ values (0.00 to 0.16 ‰) in tufa elsewhere (Fruchter et al., 2017; Liu et al., 2017). Shalev et al. (2017) analysed the $\delta^{88}\text{Sr}$ value in five tufa samples, one from France and the other from Israel, and reported values ranged from 0.00 ‰ to 0.12 ‰.

The Sr isotope fractionation during carbonate precipitation was calculated as the difference between $\delta^{88}\text{Sr}$ values in leachable (carbonate) fraction of tufa and precipitating water, denoted as (Shalev et al., 2017):

$$\Delta^{88}\text{Sr}_{\text{t-w}} = \delta^{88}\text{Sr}_{\text{tufa}} - \delta^{88}\text{Sr}_{\text{water}}$$

where t and w denote tufa and associated precipitating water, respectively.

The leachable carbonates fraction of tufa has lower $\delta^{88}\text{Sr}$ values than the dissolved Sr and $\Delta^{88}\text{Sr}_{\text{t-w}}$ ranged from -0.04 to -0.24 ‰, which are within the range of reported values (-0.02 to -0.37 ‰) (Fietzke & Eisenhauer, 2006; Halicz et al., 2008; Krabbenhöft et al., 2010; Böhm et al., 2012; Stevenson et al., 2014; Vollstaedt et al., 2014).

The $\delta^{88}\text{Sr}$ values of carbonate in tufa correlate well with tufa precipitation rate R_{calcite} ($r^2 = 0.89$), as shown in Figure 6.3a, where R_{calcite} is expressed in $10^{-9} \text{ g/cm}^2\text{s}$, and the Sr isotope fractionation $\Delta^{88}\text{Sr}_{\text{t-w}}$ is strongly correlated with the R_{calcite} , Figure 6.3b. The correlation suggests that more ^{88}Sr is incorporated into the calcite at a higher calcite precipitation rate.

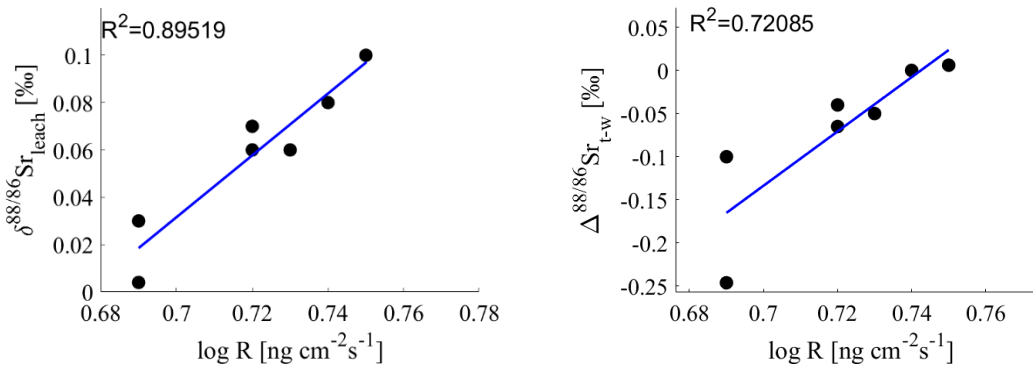


Figure 6.3: Rate dependence of a) $\delta^{88}\text{Sr}$ b) $\Delta^{88}\text{Sr}_{\text{t-w}}$ in tufa formation in the Krka river.

6.3 Identification and Quantification of Authigenic Carbonate

Water with a temperature range of 9.9°C to 23.6°C, high Ca^{2+} and HCO_3^- content and supersaturation with respect to calcite in water are ideal conditions for *in-situ* precipitation of carbonates. Moreover, $\text{SI}_{\text{calcite}}$ values ranging from 0.6 to 1.0 indicate spontaneous carbonate precipitation (Herman & Lorah, 1988). $\text{SI}_{\text{calcite}}$ ranged from 0.25 to 1.18 in previously reported data (Lojen et al., 2004; Lojen, 2007, unpublished reports). Lower SI values were measured in the colder periods of the year, meaning that the calcite precipitation during the winter and early spring is slower or does not take place at all.

As Sr co-precipitation with calcite is connected with a consistent Sr isotope fractionation (Fruchter et al., 2017; Liu et al., 2017; Shalev et al. 2017), as discussed in 6.2.2, the $\delta^{88}\text{Sr}$ of the tufa is suggested to be the identifier of authigenic carbonate.

The IsoSource (EPA) computer program was used for the calculation of mixing ratios of the authigenic and detrital carbonates. In these calculations, the proportional contributions of sources were examined in small increments (e.g. 1%) by using Sr stable isotope composition of sources (soil, bedrock, water) as of end members. The $\delta^{88}\text{Sr}$ values

of leachable fractions of soil, bedrock and tufa at respective sampling sites were used. The results are presented in Table 6.1. It should be emphasized that the presented results are a range of the most feasible combinations and not confined to a single value, such as the mean of the calculations.

Out of all calculated combinations, the most feasible source combinations for the sites K2 to K6b were 5 to 11% for bedrock, 11 to 20% for soil and 69 to 82% for authigenic carbonates. The obtained proportions are in close agreement with the possible contributions estimated by using the $^{234}\text{U}/^{238}\text{U}$ activity ratio (Rovan et al., 2021), where the distribution of sources for the sites K2 to K5b was calculated as 5 to 9% for bedrock, 11 to 26% for soil and 65 to 84% for authigenic carbonates and for the sites K6a and K6b, 9 to 13% for bedrock, 30 to 38% for soil and 41 to 61% for authigenic carbonates.

Table 6.1: Combinations of sources for each site.

Sites	Authigenic carbonates (%)	Soil (%)	Bedrock (%)
K2	80	12	8
K3	82	11	7
K4	81	14	5
K5a	77	17	6
K5b	73	19	8
K6a	72	18	10
K6b	69	20	11

6.4 Tufa as CO₂ Sink?

The precipitation rate for the whole area of waterfalls per annum was estimated from the data of the samples collected in September 2019. These are at the highest end of possible values since longer-term seasonal data showed lower SI_{calcite} in colder seasons (Lojen et al., 2004; 2009). The CO₂ storage calculations are presented in Table 6.2.

Table 6.2: Calculation of CO₂ storage capacity for the studied sites.

Sites	Precipitation rate (g/(m ² ·y))	Area of waterfalls (m ²)	Storage capacity per annum (tonnes)
K2	1540	175	0.12
K3	1670	1605	1.18
K4	1760	2094	1.62
K5	1720	35000	26.48
K6	1580	41000	28.5

The CO₂ storage in barrage tufa in the study area is calculated using the area of waterfalls and the precipitation rates (in g/(m²·s)) described in Section 4.8. The areas of waterfalls in m² were estimated using Google Earth. After converting to suitable units, the CO₂ storage was found to be in the range of 0.12 to 28.5 tonnes of CO₂/annum. Table 6.2 shows that the precipitation capacities of the waterfalls vary linearly with their area and the precipitation rate. Site K2 has the lowest storage capacity due to its smaller area and low precipitation rate, whereas site K6 has the largest area and the maximum storage capacity in spite of the lower precipitation rate.

As the samples were collected only from the waterfalls, these storage capacities do not account for the tufa precipitated in the lakes but for the barrage tufa only. It should be emphasised that the lakes formed behind tufa barriers at the Krka river are a much larger potential CO₂ sink because of their larger area and high sedimentation rates (7 to 10 mm/year, (Cukrov et al., 2013)). However, to estimate the entire 13 storage capacity of the Krka river, seasonal observations of river water and detailed analyses of lacustrine sediments would be necessary.

Chapter 7

Conclusions

The present study demonstrates a) the use of stable isotope Sr as a potential tracer for the identification and quantification of authigenic carbonates, and b) the estimation of annual CO₂ storage in recent barrage tufa in the Krka river. For this, the chemical and isotopic composition analyses of river water and tufa were performed. Based on the obtained results, the following conclusions were drawn:

- The concentration of dissolved inorganic carbon decreases downstream the river, indicating its consumption by degassing and tufa precipitation. The decreasing downstream profile of Sr and Sr/Ca ratios is influenced by the diffuse recharge of the river from the Zrmanja river. The inflow of the Sr depleted water affects the Sr concentrations more than the co-precipitation with tufa.
- The $\delta^{87}\text{Sr}$ value in tufa is lower than in the precipitating water, which is a clear indication of authigenic carbonates precipitation as described in the literature. A strong correlation was found between $\delta^{87}\text{Sr}$ and calcite precipitation rate, which is consistent with the previously published data of laboratory experiments.
- The authigenic carbonates are quantified using IsoSource (EPA). The most feasible distributions of sources include 69 to 82% for authigenic carbonates, 11 to 20% for soil carbonate and 5 to 11% for bedrock carbonate.
- Depending upon the site area and precipitation rate, the CO₂ storage capacity of the five studied waterfalls (K2 to K6) ranges from 0.16 to 38.88 tonnes per annum. These results are based on one sampling campaign only.

Generally, tufa precipitation depends on many mechanisms. In such a complex system, many different processes affect the geochemical and isotopic parameters. Some of these processes are still unexplained. Therefore, the investigation of the seasonal variability of the system, including river water, tufa and suspended materials, is required.

References

- AlKhatib, M., & Eisenhauer, A. (2017). Calcium and Strontium isotope fractionation in aqueous solutions as a function of temperature and reaction rate; I. Calcite. *Geochimica et Cosmochimica Acta*, 209, 296–319.
- Anand, P., Elderfield, H., & Conte, M. H. (2003). Calibration of Mg/Ca thermometry in planktonic foraminifera from sediment trap time series. *Paleoceanography*, 18(2), 1050.
- Anderson, T. F., & Arthur, M. A. (1983). Stable isotopes of oxygen and carbon and their application to sedimentologic and palaeoenvironmental problems. In *Stable Isotopes in Sedimentary Geology* (Eds M.A. Arthur, T.F. Anderson, I.R. Kaplan, J. Veizer and L.S. Land), Short Course Notes 10, 1.1–1.151. Tulsa, OK, USA: Society of Economic Palaeontologists and Mineralogists. SEPM Society for Sedimentary Geology.
- Andrews, J. E. (2006). Palaeoclimatic records from stable isotopes in riverine tufas; synthesis and review. *Earth-Science Reviews*, 75, 85–104.
- Andrews, J. E., & Brasier, A. T. (2005). Seasonal records of climatic change in annually laminated tufas: Short review and future prospects. *Journal of Quaternary Science*, 20, 411–421.
- Andrews, J. E., Pedley, H. M., & Dennis, P. (1994). Stable isotope record of palaeoclimatic change in a British Holocene tufa. *The Holocene*, 4, 349–355.
- Andrews, J. E., Pedley, H. M., & Dennis, P. (2000). Palaeoenvironmental records in Holocene Spanish tufas: Stable isotope approach in search of reliable climatic archives. *Sedimentology*, 47, 961–978.
- Andrews, J. E., Riding, R., & Dennis, P. (1997). The stable isotope record of environmental and climatic signals in modern terrestrial microbial carbonates from Europe. *Palaeogeography, Palaeoclimatology, Palaeoecology*, 129, 171–189.
- Appelo, C. A. J., & Postma, D. (2009). *Geochemistry, groundwater and pollution*. Taylor and Francis, Amsterdam,.
- Arenas, C., Vázquez-Urbez, M., Auqué, L. F., Sancho, C., Osácar, M. C., & Pardo, G. (2014). Intrinsic and extrinsic controls on spatial and temporal variations in modern fluvial tufa sedimentation: A thirteen-year record from a semi-arid environment. *Sedimentology*, 61, 90–132.
- Arnold, J.R., Libby, W.F. (1949). Age determinations by radiocarbon content: checks with samples of known age. *Science*, 110, 678–680.
- Arp, G., Bissett, A., Brinkmann, N., Cousin, S., de Beer, D., Friedl, T., Mohr, K. I., Neu, T. R., Reimer, A., Shiraishi, F., Stackebrandt, E., & Zippel, B. (2010). Tufa-forming biofilms of German karstwater streams: Microorganisms, exopolymers, hydrochemistry and calcification. In: *Tufas and Speleothems: Unravelling the*

- Microbial and Physical Controls (Eds H.M. Pedley and M. Rogerson). Geological Society London, 83–118.
- Arp, G., Wedemeyer, N., & Reitner, J. (2001). Fluvial Tufa Formation in a Hard-Water Creek (Deinschwanger Bach, Franconian Alb, Germany). *Facies*, 44, 1–22.
- Aufdenkampe, A. K., Mayorga, E., Raymond, P. A., Melack, J. M., Doney, S. C., Alin, S. R., Aalto, R. E., & Yoo, K. (2011). Riverine coupling of biogeochemical cycles between land, ocean, and atmosphere. *Frontiers in Ecology*, 9, 53–60.
- Avak, H., & Brand, W. A. (1995). The Finning MAT HDO-Equilibration—A fully automated H₂O/gas phase equilibration system for hydrogen and oxygen isotope analyses. Thermo Electronic Corporation. Application News, 1–13.
- Banner, J. L. (2004). Radiogenic isotopes: Systematics and applications to earth surface processes and chemical stratigraphy. *Earth-Science Reviews*, 65, 141–194.
- Bigeleisen, J., & Mayer, M. G. (1947). Calculation of equilibrium constants for isotopic exchange reactions. *The Journal of Chemical Physics*, 15, 261.
- Bisset, A., de Beer, D., Schoon, R., Shiraishi, F., Reimer, A., & Arp, G. (2008). Microbial mediation of stromatolite formation in karst-water creeks. *Limnology and Oceanography*, 53, 1159–1168.
- Böhm, F., Eisenhauer, A., Tang, J., Dietzel, M., Krabbenhöft, A., Kisakürek, B., & Horn, C. (2012). Strontium isotope fractionation of planktic foraminifera and inorganic calcite. *Geochimica et Cosmochimica Acta*, 93, 300–314.
- Bonacci, O. (1999). Water circulation in karst and determination of catchment areas: Example of the River Zrmanja. *Hydrological Sciences Journal*, 44, 373–386.
- Bonacci, O., Andrić, I., & Roje-Bonacci, R. (2017). Hydrological analysis of Skradinski buk tufa waterfall (Krka River, Dinaric karst, Croatia). *Environmental Health Sciences*, 76, 669.
- Bonacci, O., Jukić, D., & Ljubenkov, I. (2006). Definition of catchment area in karst: Case of the rivers Krcic and Krka, Croatia. *Hydrological Sciences Journal*, 51, 682–699.
- Bono, P., Dreybrodt, W., Ercole, S., Percopo, C., & Vosveck, K. (2001). Inorganic calcite precipitation in Tartare Karstic spring (Lazio, central Italy): Field measurements and theoretical prediction on depositional rates. *Environmental Geology*, 41, 305–313.
- Boussetta, S., Bassinot, F., Sabbatini, A., Caillon, N., Nouet, J., Kallel, N., Rebaubier, H., Klinkhammer, G., & Labeyrie, L. (2011). Diagenetic Mg-rich calcite in Mediterranean sediments: Quantification and impact on foraminiferal Mg/Ca thermometry. *Marine Geology*, 280(1–4), 195–204.
- Brasier, A. T., Andrews, J. E., Marca-Bell, A., & Dennis, P. (2010). Depositional continuity of seasonally laminated tufas: Implications for $\delta^{18}\text{O}$ based palaeotemperatures. *Global and Planetary Change*, 71(3), 160–167.
- Brennan, S. R., Fernandez, D. P., Mackey, G., Cerling, T. E., Bataille, C. P., Bowen, G. J., & Wooller, M. J. (2014). Strontium isotope variation and carbonate versus silicate weathering in rivers from across Alaska: Implications for provenance studies. *Chemical Geology*, 389, 167–181.
- Buhmann, D., & Dreybrodt, W. (1985). The kinetics of calcite dissolution and precipitation in geologically relevant situations of karst areas: 1. Open system. *Chemical Geology*, 48, 189–211.
- Buttman, D., & Raymond, P. A. (2011). Significant efflux of carbon dioxide from streams and rivers in the United States. *Nature Geoscience*, 4, 839–842.
- Cao, J., Yuan, D., Groves, C., Huang, F., Yang, H., & Lu., Q. (2012). Carbon fluxes and sinks: The consumption of atmospheric and soil CO₂ by carbonate rock dissolution. *Acta Geologica Sinica-English Edition*, 86, 963–972.
- Capezzuoli, E., Gandin, A., & Pedley, M. (2014). Decoding tufa and travertine (fresh water carbonates) in the sedimentary record: The state of the art. *Sedimentology*, 61, 1–21.

- Capo, R. C., Stewart, B. W., & Chadwick, O. A. (1998). Strontium isotopes as tracers of ecosystem processes: Theory and methods. *Geoderma*, 82, 197–225.
- Catanzaro, E. L., Murphy, T. J., Garner, E. L., & Shields, W. R. (1966). Absolute isotopic abundance ratios and atomic weight of magnesium. *J. Res. Natl. Bur. Stand.*, 70A, 453–458.
- Chan, L. H. (1987). Lithium isotope analysis by thermal ionization mass- spectrometry of lithium tetraborate. *Anal. Chem.*, 59, 2662–2665.
- Chao, H. C., You, C. F., Liu, H. C., & Chung, C. H. (2013). The origin and migration of mud volcano fluids in Taiwan: Evidence from hydrogen, oxygen, and strontium isotopic compositions. *Geochimica et Cosmochimica Acta*, 114, 29–51.
- Chao, H. C., You, C. F., Liu, H. C., & Chung, C. H. (2015). Evidence for stable Sr isotope fractionation by silicate weathering in a small sedimentary watershed in southwestern Taiwan. *Geochimica et Cosmochimica Acta*, 165, 324–341.
- Charlier, B. L. A., Nowell, G. M., Parkinson, I. J., Kelley, S. P., Pearson, D. G., & Burton, K. W. (2012). High temperature strontium stable isotope behaviour in the early solar system and planetary bodies. *Earth and Planetary Science Letters*, 329, 31–40.
- Chen, J., Zhang, D. D., Wang, S., Xiao, T., & Huang, R. (2004). Factors controlling tufa deposition in natural waters at waterfall sites. *Sedimentary Geology*, 166, 353–366.
- Clark, I. D., & Fritz, P. (1997). *Environmental Isotopes in Hydrogeology*. Lewis Publishers.
- Cole, J. J., Pairie, Y. T., Caraco, N. F., McDowell, W. H., Tranvik, L. J., Striegl, R. G., Duarte, C. M., Kortelainen, P., Downing, J. A., Middelburg, J. J., & Melack, J. (2007). Plumbing the global carbon cycle: Integrating inland waters into the terrestrial carbon budget. *Ecosystems*, 10(1), 172–185.
- Colombié, C., Lécuyer, C., & Strasser, A. (2011). Carbon- and oxygen-isotope records of palaeoenvironmental and carbonate production changes in shallow-marine carbonates (Kimmeridgian, Swiss Jura). *Geol. Mag.*, 148, 133–153.
- Coplen, T. B., Wildman, J. D., & Chen, J. (1991). Improvements in the gaseous hydrogen-water equilibration technique for hydrogen isotope-ratio analysis. *Anal. Chem.*, 63, 910–912.
- Coplen, T. D. (2007). Calibration of the calcite–water oxygen-isotope geothermometer at Devils Hole, Nevada, a natural laboratory. *Geochimica et Cosmochimica Acta*, 71, 3948–3957.
- Craig, H. (1965). The measurement of oxygen isotope paleotemperatures. In: *Stable Isotopes in Oceanographic Studies and Paleotemperatures* (Ed. E. Tongiorgi), Lab. Geol. Nucl. Pisa, 3, 23.
- Cukrov, N., Cmok, P., Mlakar, M., & Omanović, D. (2008). Spatial distribution of trace metals in the Krka River, Croatia: An example of the self-purification. *Chemosphere*, 72, 1559–1566.
- Cukrov, N., Cuculic, V., Barišić, D., Lojen, S., Mikelić, I. L., Višnja, O., Vdović, N., Fiket, Ž., & Čermelj, B. (2013). Elemental and isotopic records in recent fluvio-lacustrine sediments in karstic river Krka, Croatia. *Journal of Geochemical Exploration*, 134, 51–60.
- Cukrov, N., Topić, N., Omanović, D., Lojen, S., Bura-Nakić, E., Vojvodić, V., & Pižeta, I. (2009). Anthropogenic and natural influences on the Krka River (Croatia) evaluated by multivariate statistical analysis. *ITI 2009. 31st Int. Conf. on Information Technology Interfaces*, Cavtat, Croatia.
- Dabkowski, J., Limondin-Lozouet, N., Antoine, P., Andrews, J., Marca-Bell, A., & Robert, V. (2012). Climatic variations in MIS 11 recorded by stable isotopes and trace elements in a French tufa (La Celle, Seine Valley). *Journal of Quaternary Science*, 27, 790–799.

- Daëron, M., Drysdale, R. N., Peral, M., Huyghe, D., Blamart, D., Coplen, T. B., Lartaud, F., & Zanchetta, G. (2019). Most Earth-surface calcites precipitate out of isotopic equilibrium. *Nat Commun*, 10, 429.
- Das, D. K. (2008). Decomposition of geological materials for trace elements analysis. In: *Trans Analysis* (Narosa, New Delhi), 1–29.
- Decho, A. W. (2010). Overview of biopolymer-induced mineralization: What goes on in biofilms? *Ecological Engineering*, 36, 137–144.
- Dedić, Ž., Ilijanić, N., & Miko, S. (2018). A mineralogical and petrographic study of evaporites from the Mali Kukor, Vranjkovići, and Slane Stine deposits (Upper Permian, Dalmatia, Croatia). *Geologoa Croatica*, 7, 19–28.
- Deines, P., Langmuir, D., & Harmon, R. S. (1974). Stable carbon isotope ratios and the existence of a gas phase in the evolution of carbonate ground waters. *Geochimica et Cosmochimica Acta*, 38, 1147–1164.
- Delaney, M. L., Be, A. W. H., & Boyle, E. A. (1985). Li, Sr, Mg and Na in foraminiferal calcite shells from laboratory culture, sediment traps, and sediment cores. *Geochimica et Cosmochimica Acta*, 49, 1327–1341.
- Dietzel, M., Tang, J., Leis, A., & Köhler, S. J. (2009). Oxygen isotopic fractionation during inorganic calcite precipitation — Effects of temperature, precipitation rate and pH. *Chemical Geology*, 268(1–2), 107–115.
- Dlugokencky, E., & Tans, P. (2019). Trends in atmospheric carbon dioxide, National Oceanic & Atmospheric Administration, Earth System Research Laboratory (NOAA/ESRL),.
- Dorale, J. A., Edwards, R. L., Ito, E., & Gonzalez, L. A. (1998). Climate and vegetation history of the midcontinent from 75 to 25 ka: A speleothem record from Crevice Cave, Missouri, USA. *Science*, 282, 1871–1874.
- Douthitt, C. B. (2008). The evolution and applications of multicollector ICPMS (MC-ICPMS). *Anal. Bioanal. Chem.*, 390, 437–440.
- Dreybrodt, W. (1988). Modelling the Kinetics of Calcite Dissolution and Precipitation in Natural Environments of Karst Areas. In: *Processes in karst systems, physics, chemistry, and geology.* (pp. 140–182). Springer-Verlag.
- Dreybrodt, W. (2019). Physics and chemistry of CO₂ outgassing from a solution precipitating calcite to a speleothem: Implication to ¹³C, ¹⁸O, and clumped ¹³C¹⁸O isotope composition in DIC and calcite. *Acta Carsologica*, 48, 59–68.
- Dreybrodt, W., & Buhmann, D. (1991). Mass transfer model for dissolution and precipitation of calcite from solutions in turbulent motion. *Chemical Geology*, 90, 107–122.
- Dreybrodt, W., Buhmann, D., Michaelis, J., & Usdowski, E. (1992). Geochemically controlled calcite precipitation by CO₂ outgassing: Field measurements of precipitation rates in comparison to theoretical predictions. *Chemical Geology*, 97, 285–294.
- Dupraz, C., Pamela Reid, R., Braissant, O., Decho, A. W., Norman, R. S., & Visscher, P. T. (2009). Processes of carbonate precipitation in modern microbial mats. *Earth-Science Reviews*, 96(3), 141–162.
- Ehleringer, J. R., Buchmann, N., & Flanagan, L. B. (2000). Carbon isotope ratios in belowground carbon cycle processes. *Ecol. Appl.*, 10, 412–422.
- Elderfield, H., Yu, J., Anand, P., Kiefer, T., & Nyland, B. (2006). Calibrations for benthic foraminiferal Mg/Ca paleothermometry and the carbonate ion hypothesis. *Earth and Planetary Science Letters*, 250(3–4), 633–649.
- Emeis, K. C., Richnow, H. H., & Kempe, S. (1987). Travertine formation in Plitvice National Park, Yugoslavia: Chemical versus biological control. *Sedimentology*, 34, 595–609.

- Epstein, S., Buchsbaum, R., Lowenstam, H., & Urey, H. C. (1951). Carbonate-water isotopic temperature scale. *Geol. Soc. Am. Bull.*, 62, 417–426.
- Epstein, S., & Mayeda, T. K. (1953). Variation of ^{18}O content of waters from natural sources. *Geochimica et Cosmochimica Acta*, 4, 213–224.
- Esser, G., Kattge, J., & Sakalli, A. (2011). Feedback of carbon and nitrogen cycles enhances carbon sequestration in the terrestrial biosphere. *Global Change Biology*, 17, 819–842.
- Feng, W., Banner, J. L., Guilfoyle, A. L., Musgrove, M., & James, E. W. (2012). Oxygen isotopic fractionation between drip water and speleothem calcite: A 10-year monitoring study, central Texas, USA. *Chemical Geology*, 304, 53–67.
- Fietzke, J., & Eisenhauer, A. (2006). Determination of temperature-dependent stable strontium isotope ($^{88}\text{Sr}/^{86}\text{Sr}$) fractionation via bracketing standard MC-ICP-MS. *Geochemistry Geophysics Geosystems*, 7(8). <https://doi.org/10.1029/2006GC001243>.
- Filipović Marijić, V., Kapetanović, D., Ka Dragun, Z., Valić, D., Krasnići, N., Redžović, Z., Grgić, I., Žunić, J., Kružlicová, D., Nemeček, P., Ivanković, D., Vardić Smrzlić, I., & Erk, M. (2018). Influence of technological and municipal waste waters on vulnerable karst riverine system, Krka river in Croatia. *Environmental Science and Pollution Research*, 25, 4715–4727.
- Filipović Marijić, V., Lajtner, J., Grgić, I., & Redžović, Z. (n.d.). Procjena Antropogenih utjecaja na rijeku Krku i potencijalne opasnosti za Nacionalni park Krka (Assessment of anthropogenic influences on Krka river and potential risk for the Krka national park). University of Zagreb, Faculty of Science, Rector's Award; Accessible at <https://www.bib.irb.hr/859440>.
- Finlay, J. C., & Kendall, C. (2007). Stable isotope tracing of temporal and spatial variability in organic matter sources to freshwater ecosystems. In: *Stable Isotopes in Ecology and Environmental Science*. Blackwell Publishing Ltd, Singapore, 283–333.
- Fohlmeister, J., Arps, G., Spötl, C., Schröder-Ritzrau, A., Plessen, B., Günter, C., Frank, N., & Trüssel, M. (2018). Carbon and oxygen isotope fractionation in the water-calcite-aragonite system. *Geochimica et Cosmochimica Acta*, 235, 127–139.
- Ford, T. D., & Pedley, H. M. (1996). A review of tufa and travertine deposits of the world. *Earth-Science Reviews*, 41, 117–175.
- Fouke, B. W., Farmer, J. D., Des Marais, D. J., Pratt, L., Strucchio, N. c., Burns, P. C., & Discipulo, M. K. (2000). Depositional facies and aqueous—Solid geochemistry of travertine depositing hot springs (Angel Terrace, Mammoth Hot Springs, Yellowstone National Park, U.S.A.). *Journal of Sedimentary Research*, 70, 565–585.
- Friedman, I., & O'Neil, J. R. (1977). Compilation of stable isotope fractionation factors of geochemical interest. In: *Data of Geochemistry*. U. S. Geological Survey, Washington, 1–12.
- Fruchter, N., Eisenhauer, A., Dietzel, M., Fietzke, J., Böhm, F., Montaga, P., Stein, M., Lazar, B., Rodolfo-Metalpa, R., & Erez, J. (2016). $^{88}\text{Sr}/^{86}\text{Sr}$ fractionation in inorganic aragonite and in corals. *Geochimica et Cosmochimica Acta*, 178, 268–280.
- Fruchter, N., Lazar, B., Nishiri, A., Almogi-Labin, A., Eisenhauer, A., Shlevin, Y. B., & Stein, M. (2017). $^{87}\text{Sr}/^{86}\text{Sr}$ fractionation and calcite accumulation rate in the Sea of Galilee. *Geochimica et Cosmochimica Acta*, 215, 17–32.
- Gaillardet, J., Dupré, B., Louvat, P., & Allegre, C. J. (1999). Global silicate weathering and CO_2 consumption rates deduced from the chemistry of large rivers. *Chemical Geology*, 159, 3–30.
- Galy, A., France-Lanord, C., & Derry, L. A. (1999). The strontium isotopic budget of Himalayan Rivers in Nepal and Bangladesh. *Geochimica et Cosmochimica Acta*, 63, 1905–1925.

- Garnett, E. R., Andrews, J. E., Preece, R. C., & Dennis, P. F. (2004). Climatic change recorded by stable isotopes and trace elements in a British Holocene tufa. *J. Quat. Sci.*, 19, 251–262.
- Gieskes, J. M. (1974). The alkalinity-total carbon dioxide system in seawater. In E. D. Goldberg (Ed.), *Marine Chemistry of the Sea* (Vol. 5, pp. 123–151).
- Gray, W. R., & Evans, D. (2019). Nonthermal Influences on Mg/Ca in Planktonic Foraminifera: A Review of Culture Studies and Application to the Last Glacial Maximum. *Paleoceanography and Paleoclimatology*, 34, 306–315.
- Green, G. R., & Taheri, J. (1992). Stable isotopes and geochemistry as exploration indicators. *Geological Survey Bulletin*, 70, 84–91.
- Guo, W. (2008). Carbonate clumped isotope thermometry: Application to carbonaceous chondrites and effects of kinetic isotope fractionation. *California Institute of Technology*.
- Halicz, L., Segal, I., Fruchter, N., Stein, M., & Lazar, B. (2008). Strontium stable isotopes fractionate in the soil environments? *Earth and Planetary Science Letters*, 272, 406–411.
- Hatten, J. A., Goñi, B. A., & Wheatcroft, R. A. (2012). Chemical characteristics of particulate organic matter from a small, mountainous river system in the Oregon Coast Range, USA. *Biogeochemistry*, 107, 43–66.
- Hays, P. D., & Grossman, E. L. (1991). Oxygen isotopes in meteoric calcite cements as indicators of continental paleoclimate. *Geology*, 19, 441–444.
- Heiman, A., & Sass, E. (1989). Travertines in the northern Hula Valley, Israel. *Sedimentology*, 36, 95–108.
- Herman, J. S., & Lorah, M. M. (1988). Calcite precipitation rates in the field: Measurement and prediction for a travertine-depositing stream. *Geochimica et Cosmochimica Acta*, 52, 2347–2355.
- Hoef, J. (2009). *Stable isotope geochemistry*. Springer-Verlag, Berlin, Heidelberg.
- Hope, D., Palmer, S. M., Billett, M. F., & Dawson, J. J. (2004). Variations in dissolved CO₂ and CH₄ in a first-order stream and catchment: An investigation of soil-stream linkages. *Hydrological Processes*, 18, 3255–3275.
- Hori, M., Hoshino, K., Okumura, K., & Kano, A. (2008). Seasonal patterns of carbon chemistry and isotopes in tufa depositing groundwaters of southwestern Japan. *Geochimica et Cosmochimica Acta*, 72, 480–492.
- Horvatinčić, N., Bronić, I. K., & Obelić, B. (2003). Differences in the ¹⁴C age, δ¹³C and δ¹⁸O of Holocene tufa and speleothem in the Dinaric Karst. *Palaeogeography, Palaeoclimatology, Palaeoecology*, 193, 139–157.
- Horvatinčić, N., Čalić, R., & Geyh, M. (2000). Interglacial Growth of Tufa in Croatia. *Quaternary Research*, 53(2), 185–195.
- Hotchkiss, E. R., Hall, R. O., Sponseller, R. A., Butman, D., Klaminder, J., Laudon, H., Roswall, M., & Karlsson, J. (2015). Sources of and processes controlling CO₂ emissions change with the size of streams and rivers. *Nature Geoscience*, 8, 696–699.
- Hounslow, A. W. (1995). *Water quality data: Analysis and Interpretation*. Lewis Publishers.
- Huang, Y., & Fairchild, I. J. (2001). Partitioning of Sr²⁺ and Mg²⁺ into calcite under karst-analogue experimental conditions. *Geochimica et Cosmochimica Acta*, 65, 47–62.
- Ihlenfeld, C., Norman, M. D., Gagan, M. K., Drysdale, R. N., Maas, R., & Webb, J. (2003). Climatic significance of seasonal trace element and stable isotope variations in a modern freshwater tufa. *Geochimica et Cosmochimica Acta*, 67, 2341–2357.
- Janssen, A., Swennen, R., Podoor, N., & Keppens, E. (1999). Biological and diagenetic influence in Recent and fossil tufa deposits from Belgium. *Sedimentary Geology*, 126, 75–95.

- Jimenez-Lopez, C., Caballero, E., Huertas, F. J., & Romanek, C. S. (2001). Chemical, mineralogical and isotope behavior, and phase transformation during the precipitation of calcium carbonate minerals from intermediate ionic solution at 25 °C. *Geochimica et Cosmochimica Acta*, 65, 3219–3231.
- Johnson, C. M., Beard, B. L., & Albarède, F. (2004). Overview and General Concepts. *Reviews in Mineralogy and Geochemistry*, 55(1), 1–24.
- Kanduč, T., Ogrinc, N., & Mrak, T. (2007b). Characteristics of suspended matter in the River Sava watershed, Slovenia. *Isotopes in Environmental and Health Studies*, 43, 369–386.
- Kanduč, T., Szramek, K., Ogrinc, N., & Walter, L. M. (2007a). Origin and cycling of riverine inorganic carbon in the Sava River watershed (Slovenia) inferred from major solutes and stable carbon isotopes. *Biogeochemistry*, 86, 137–154.
- Kano, A., Matsuoka, J., Kojo, T., & Fujii, H. (2003). Origin of annual laminations in tufa deposits, southwest Japan. *Palaeogeography, Palaeoclimatology, Palaeoecology*, 191(2), 243–262.
- Kawai, T., Kano, A., Matsuoka, J., & Ihara, T. (2006). Seasonal variation in water chemistry and depositional processes in a tufa-bearing stream in SW-Japan, based on 5 years of monthly observations. *Chemical Geology*, 232, 33–53.
- Kendall, C., & Coplen, T. B. (2001). Distribution of oxygen-18 and deuterium in river waters across the United States. *Hydrological Processes*, 15, 1363–1393.
- Kendall, C., & McDonnell, J. J. (1998). *Isotope tracers in catchment hydrology*. Elsevier Science Ltd.
- Kim, S. T., & O’Neil, J. R. (1997). Equilibrium and nonequilibrium oxygen isotope effects in synthetic carbonates. *Geochimica et Cosmochimica Acta*, 61, 3461–3475.
- Krabbenhöft, A., Eisenhauer, A., Böhm, F., Vollstaedt, H., Fietzke, J., Liebetrau, V., Augustin, N., Peucker-Ehrenbrink, B., Müller, M. N., Horn, C., Hansen, B. T., Nolte, N., & Wallman, K. (2010). Constraining the marine strontium budget with natural strontium isotope fractionations ($^{87}\text{Sr}/^{86}\text{Sr}^*$, $\delta^{88/86}\text{Sr}$) of carbonates, hydrothermal solutions and river waters. *Geochimica et Cosmochimica Acta*, 74(14), 7097–4109.
- Krabbenhöft, A., Fietzke, J., Eisenhauer, A., Liebetrau, V., Böhm, F., & Vollstaedt, H. (2009). Determination of radiogenic and stable strontium isotope ratios ($^{87}\text{Sr}/^{86}\text{Sr}$, $\delta^{88/86}\text{Sr}$) by thermal ionization mass spectrometry applying an $^{87}\text{Sr}/^{84}\text{Sr}$ double spike. *Journal of Analytical Atomic Spectrometry*, 24, 1267–1271.
- Kulušić, A., & Borojević Šoštarić, S. (2014). Dinaride evaporite mélange: Diagenesis of the Kosovo polje evaporites. *Geologia Croatica*, 67, 59–74.
- Leybourne, M. I., Betcher, R. N., McRitchie, W. D., Kaszycki, C. A., & Boyle, D. R. (2009). Geochemistry and stable isotopic composition of tufa waters and precipitates from the Interlake Region, Manitoba, Canada: Constraints on groundwater origin, calcitization, and tufa formation. *Chemical Geology*, 260, 221–233.
- Liu, C., Wang, Z., & Macdonald, F. A. (2018). Sr and Mg isotope geochemistry of the basal ediacaran cap limestone sequence of Mongolia: Implications for carbonate diagenesis, mixing of glacial meltwaters, and seawater chemistry in the aftermath of Snowball Earth. *Chemical Geology*, 491, 1–13.
- Liu, C., Wang, Z., & Raub, T. D. (2013). Geochemical constraints on the origin of Marinoan cap dolostones from Nuccaleena Formation, South Australia. *Chemical Geology*, 351, 95–104.
- Liu, C., Wang, Z., Raub, T. D., Macdonald, F. A., & Evans, D. A. D. (2014a). Neoproterozoic cap-dolostone deposition in stratified glacial meltwater plume. *Earth and Planetary Science Letters*, 44, 22–32.
- Liu, H. C., You, C. F., Zhou, H., Huang, K. F., Chung, C. H., Huang, W. J., & Tang, J. (2017). Effect of calcite precipitation on stable strontium isotopic composition:

- Insights from riverine and pool waters in a karst cave. *Chemical Geology*, 456, 85–97.
- Liu, Z., & Dreybrodt, W. (1997). Dissolution kinetics of calcium carbonate minerals in H₂O-CO₂ solutions in turbulent flow: The role of the diffusion boundary layer and the slow reaction H₂O + CO₂ → H⁺ + HCO₃⁻. *Geochimica et Cosmochimica Acta*, 61, 2879–2889.
- Liu, Z., Svensson, U., Dreybrodt, W., Daoxian, Y., & Buhmann, D. (1995). Hydrodynamic control of inorganic calcite precipitation in Huanglong Ravine, China: Field measurements and theoretical prediction of deposition rates. *Geochimica et Cosmochimica Acta*, 59, 3087–3097.
- Lojen, S. (2007). Geochemical investigation of tufa barriers in the Krka National Park, Croatia. Unpublished data.
- Lojen, S., Dolenc, T., Vokal, B., Cukrov, N., Mihelčić, G., & Papesch, W. (2004). C and O stable isotope variability in recent freshwater carbonates (River Krka, Croatia). *Sedimentology*, 51, 361–375.
- Lojen, S., Trkov, A., Ščančar, J., Vázquez-Navarro, J., & Cukrov, N. (2009). Continuous 60-year stable isotopic and earth-alkali element records in a modern laminated tufa (Jaruga, river Krka, Croatia): Implications for climate reconstruction. *Chemical Geology*, 258, 242–250.
- Lojen, S., Vokal, B., & Žigon, S. (2002). Geochemical investigation of tufa barriers in the Krka National Park, Croatia. Unpublished data.
- Lorens, R. B. (1981). Sr, Cd, Mn and Co distribution coefficients in calcite as a function of calcite precipitation rate. *Geochimica et Cosmochimica Acta*, 45, 553–561.
- Ma, J.-L., Wei, G.-J., Liu, Y., Ren, Z.-Y., Xu, Y.-G., & Yang, Y.-H. (2013). Precise measurement of stable ($\delta^{88/86}\text{Sr}$) and radiogenic ($^{87}\text{Sr}/^{86}\text{Sr}$) strontium isotope ratios in geological standard reference materials using MC-ICP-MS. *Chinese Science Bulletin*, 58, 3111–3118.
- Mackenzie, F. T., & Lerman, A. (2006). *Carbon in the geobiosphere: Earth's outer shell*. Springer.
- Mamudžić, P. (1971). Osnovna geološka karta SFRJ 1: 100 000, list Šibenik (Basic Geological Map of SFT Yugoslavia, page Šibenik). Geological Survey of Yugoslavia, Belgrade
- Marčenko, E., Srdoč, D., Golubić, S., Pezdič, J., & Head, M. J. (1988). Carbon Uptake in Aquatic Plants Deduced From Their Natural ¹³C and ¹⁴C Content. *Radiocarbon*, 31, 785–794.
- Marić, I., Šiljeg, A., Cukrov, N., Roland, V., & Domazetović, F. (2020). How fast does tufa grow? Very high-resolution measurement of the tufa growth rate on artificial substrates by the development of a contactless image-based modelling device. *Earth Surf. Process. Landforms*, 45, 2331–2349.
- Marker, M. E. (1988). Tufa deposits of southern Africa: In *Palaeoecology of Africa and the Surrounding Islands* (Vol. 19, pp. 377–389). Balkema, Rotterdam,.
- Matsuoka, J., Kano, A., Oba, T., Watanabe, T., Sakai, S., & Seto, K. (2001). Seasonal variation of stable isotopic compositions recorded in a laminated tufa, SW Japan. *Earth and Planetary Science Letters*, 192, 31–44.
- Mayer, B. (1998). Potential and limitations of using sulfur isotope abundance ratios as an indicator for natural and anthropogenic induced environmental change. In: *Isotope Techniques in the Study of Past and Current Environmental Changes in the Hydrosphere and the Atmosphere*. IAEA, Vienna, 1998, 423–435.
- McCrea, J. M. (1950). On the isotopic chemistry of carbonates and a paleotemperature scale. *The Journal of Chemical Physics*, 18, 849.

- McKinney, C. R., McCrea, J. M., Epstein, S., Allen, H. A., & Urey, H. C. (1950). Improvements in Mass Spectrometers for the Measurement of Small Differences in Isotope Abundance Ratios. *Review of Scientific Instruments*, 21, 724–730.
- Merz-Preiß, M., & Riding, R. (1999). Cyanobacterial tufa calcification in two freshwater streams: Ambient environment, chemical thresholds and biological processes. *Sedimentary Geology*, 126, 103–124.
- Michener, R., & Lajtha, K. (2007). *Stable isotopes in ecology and environmental science* (2nd ed.). Blackwell Publishing.
- Miyajima, T., Yamada, Y., & Hanba, Y. T. (1995). Determining the stable isotope ratio of total dissolved inorganic carbon in lake water by GC/C/IRMS. *Limnology and Oceanography*, 40, 994–1000.
- Mokadem, F., Parkinson, I. J., Hathorne, E. C., Anand, P., Allen, J. T., & Burton, K. W. (2015). High-precision radiogenic strontium isotope measurements of the modern and glacial ocean: Limits on glacial–interglacial variations in continental weathering. *Earth and Planetary Science Letters*, 415, 111–120.
- Mook, W. G. (2000). *Environmental isotopes in the hydrological cycle: Principles and applications*. IAEA and UNESCO, Vienna.
- Mook, W. G., Bommerson, J. C., & Staverman, W. H. (1974). Carbon isotope fractionation between dissolved bicarbonate and gaseous carbon dioxide. *Earth and Planetary Science Letters*, 22, 169–176.
- Not, C., Thibodeau, B., & Yokoyama, Y. (2018). Incorporation of Mg, Sr, Ba, U, and B in High-Mg Calcite Benthic Foraminifers Cultured Under Controlled pCO₂. *Geochemistry Geophysics Geosystems*, 19, 83–98.
- O’Brien, G. R., Kaufman, D. S., Sharp, W. D., Atudorei, V., Parnell, R. A., & Crossey, L. J. (2006). Oxygen isotope composition of annually banded modern and mid- Holocene travertine and evidence of paleomonsoon floods, Grand Canyon, Arizona, USA. *Quaternary Research*, 65, 366–379.
- Oliva, P., Viers, J., & Dupré, B. (2003). Chemical weathering in granitic environments. *Chemical Geology*, 202, 225–256.
- O’Neil, J. R., Clayton, R. N., & Mayeda, T. K. (1969). Oxygen isotope fractionation in divalent metal carbonates. *The Journal of Chemical Physics*, 51, 5547.
- Ortiz, J.E., Torres, T., Delgado, A., Reyes, E., Diaz-Bautista, A., 2009. A review of the Tagus river tufa deposits (central Spain): age and palaeoenvironmental record. *Quat. Sci. Rev.* 28, 947–963.
- Osácar, M. C., Arenas, C., Vázquez-Urbez, M., Sancho, C., Auqué, L. F., & Pardo, G. (2013). Environmental factors controlling the $\delta^{13}\text{C}$ and $\delta^{18}\text{O}$ of recent fluvial tufas: A 12-year record from the monasterio de Piedra natural park (NE Iberian Peninsula). *Journal of Sedimentary Research*, 83, 309–322.
- Ouyang, Y., Nkedi-Kizza, P., Wu, Q. T., Shinde, D., & Huang, C. H. (2006). Assessment of seasonal variations in surface water quality. *Water Research*, 40, 3800–3810.
- Palmer, M. R., & Edmond, J. M. (1992). Controls over the strontium isotope composition of river water. *Geochimica et Cosmochimica Acta*, 56, 2099–2111.
- Parkhurst, D. L., & Appelo, C. A. J. (1999). User’s guide to PHREEQC (version 2)—A computer program for speciation, batch-reaction, one-dimensional transport, and inverse geochemical calculations. In: *Water-Resources Investigations Report 99-4259*. U. S. Geological Survey, Denver, 1–312.
- Pazdur, A., Pazdur, M. F., Starkel, L., & Szulc, J. (1988). Stable isotopes of Holocene calcareous tufa in southern Poland as paleoclimatic indicators. *Quaternary Research*, 30, 177–189.
- Pearce, C. R., Parkinson, I. J., Gaillardet, J., Charlier, B. L. A., Mokadem, F., & Burton, K. W. (2015). Reassessing the stable ($\delta^{88/86}\text{Sr}$) and radiogenic ($^{87}\text{Sr}/^{86}\text{Sr}$) strontium

- isotopic composition of marine inputs. *Geochimica et Cosmochimica Acta*, 157, 125–146.
- Pedley, M. (1992). Freshwater (phytoherm) reefs: The role of biofilms and their bearing on marine reef cementation. *Sedimentary Geology*, 79, 255–274.
- Pedley, M. (2014). The morphology and function of thrombolitic calcite precipitating biofilms: A universal model derived from fresh water mesocosm experiments. *Sedimentology*, 61, 22–40.
- Pella, E., & Colombo, B. (1978). Simultaneous CHN and S microdetermination by combustion and gas chromatography. *Microchimica Acta*, 69, 271–286.
- Peña, J. L., Sancho, C., & Lozano, M. V. (2000). Climatic and tectonic significance of Pleistocene and Holocene tufa deposits in the Mijares River canyon, eastern Iberian range, Northeastern Spain. *Earth Surf. Proc. Land.*, 25, 1403–1417.
- Pentecost, A. (2005). *Travertine*. Springer-Verlag, Berlin, Heidelberg.
- Polag, D., Scholz, D., Mühlinghaus, C., Spötl, C., Schröder-Ritzrau, A., Segl, M., & Mangini, A. (2010). A. Stable isotope fractionation in speleothems: Laboratory experiments. *Chemical Geology*, 279(1–2), 31–39.
- Quary, P. D., Tilbrook, B., & Wong, C. S. (1992). Oceanic uptake of fossil fuel CO₂: Carbon-13 evidence. *Science*, 256, 74–79.
- Raddatz, J., Liebetrau, V., Rüggeberg, A., Hathorne, E. C., Krabbenhoft, A., Eisenhauer, A., Böhm, F., Vollstaedt, H., Fietzke, J., López Correa, M., Freiwald, A., & Dullo, W. C. (2013). Stable Sr-isotope, Sr/Ca, Mg/ Ca, Li/Ca and Mg/Li ratios in the scleractinian cold-water coral *Lophelia pertusa*. *Chemical Geology*, 352, 143–152.
- Rassmann, J., Lansard, B., Pozzato, L., & Rabouille, C. (2016). Carbonate chemistry in sediment porewaters of the Rhône River delta driven by early diagenesis (northwestern Mediterranean). *Biogeosciences*, 13, 5379–5394.
- Raymond, P. A., Hartmann, J., Lauerwald, R., Sobek, S., McDonald, C., Hoover, M., Butman, D., Striegl, R., Mayorga, E., Humborg, C., Kortelainen, P., Durr, H., Meybeck, M., Ciais, P., & Guth, P. (2013). Global carbon dioxide emissions from inland waters. *Nature*, 503, 355–359.
- Richey, J. E. (2005). Global River Carbon Biogeochemistry. In: *Encyclopedia of Hydrological Sciences*.
- Riding, R. (1979). Origin and diagenesis of lacustrine algal bioherms at the margin of the Ries Crater, Upper Miocene, southern Germany. *Sedimentology*, 26, 645–680.
- Ritter, S. M., Isenbeck-Schröter, M., Schröder-Ritzrau, A., Scholz, C., Rheinberger, S., Höfle, B., & Frank, N. (2018). Trace element partitioning in fluvial tufa reveals variable portions of biologically influenced calcite precipitation. *Geochimica et Cosmochimica Acta*, 225, 176–191.
- Rogerson, M., Pedley, H. M., & Wadhawan, J. D. (2014). Linking mineralisation process and sedimentary product in terrestrial carbonates using a solution thermodynamic approach. *Earth Surface Dynamics*, 2, 197–216.
- Rogerson, M., Pedley, H. M., Wadhawan, J. D., & Middleton, R. (2008). New insights into biological influence on the geochemistry of freshwater carbonate deposits. *Geochimica et Cosmochimica Acta*, 72, 4976–4987.
- Romanek, C. S., Grossman, E. L., & Morse, J. W. (1992). Carbon isotopic fractionation in synthetic aragonite and calcite: Effects of temperature and precipitation rate. *Geochimica et Cosmochimica Acta*, 56, 419–430.
- Rovan, L., Lojen, S., Zuliani, T., Kanduč, T., Petrič, M., Horvat, B., & Štok, M. (2020). Comparison of Uranium Isotopes and Classical Geochemical Tracers in Karst Aquifer of Ljubljana River catchment (Slovenia). *Water*, 12(7), 2064.
- Rovan, L., Zuliani, T., Horvat, B., Kanduč, T., Vreča, P., Jamil, Q., Čermelj, B., Nakić, E. B., Cukrov, N., Štok, M., & Lojen, S. (2021). Uranium isotopes in tufa: A possible

- tracer of environmental processes? Example of Krka River, Croatia. *Science of the Total Environment* (In Review).
- Saulnier, S., Rollion-Bard, C., Vigier, N., & Chaussidon, M. (2012). Mg isotope fractionation during calcite precipitation: An experimental study. *Geochimica et Cosmochimica Acta*, 91, 75–91.
- Saunders, P., Rogerson, M., Wadhawan, J. D., Greenway, G., & Pedley, H. M. (2014). Mg/Ca ratios in freshwater microbial carbonates: Thermodynamic, kinetic and vital effects. *Geochimica et Cosmochimica Acta*, 147, 107–118.
- Schrag, D. P., Higgins, J. A., Macdonald, F. A., & Johnston, D. T. (2013). Authigenic Carbonate and the History of the Global Carbon Cycle. *Science*, 339, 540–543.
- Shalev, N., Gavrieli, I., Halicz, L., Sandler, A., Stein, M., & Lazar, B. (2017). Enrichment of ^{88}Sr in continental waters due to calcium carbonate precipitation. *Earth and Planetary Science Letters*, 459, 381–393.
- Shalev, N., Segal, I., Lazar, B., Gavrieli, I., Fietzke, J., Eisenhauer, A., & Halicz, L. (2013). Precise determination of $\delta^{88/86}\text{Sr}$ in natural samples by double-spike MC-ICP-MS and its TIMS verification. *Journal of Analytical Atomic Spectrometry*, 28, 940–944.
- Shand, P., Darbyshire, D. P. F., Love, A. J., & Edmunds, W. M. (2009). Sr isotopes in natural waters: Applications to source characterisation and water–rock interaction in contrasting landscapes. *Applied Geochemistry*, 24, 574–586.
- Sharp, Z. D. (2007). *Principles of Stable Isotope Geochemistry*. Pearson Prentice Hall.
- Shiraishi, F., Bisset, A., de Beer, D., Reimer, A., & Arp, G. (2008). Photosynthesis, Respiration and Exopolymer Calcium-Binding in Biofilm Calcification (Westerhöfer and Deinschwanger Creek, Germany). *Geomicrobiology Journal*, 25, 83–94.
- Smieja-Król, B., Bauerek, A., & Bebek, M. (2017). Main and Trace Element Distribution in Slag-Leachate-Tufa System Precipitate. *Pol. J. Environ. Stud.*, 26, 287–292.
- Spötl, C. (2005). A robust and fast method of sampling and analysis of $\delta^{13}\text{C}$ of dissolved inorganic carbon in ground waters. *Isotopes in Environ Health Studies*, 41, 217–221.
- Stevenson, E. I., Burton, K. W., Mokadem, F., Parkinson, I. J., Anand, P., & Hathorne, E. C. (2010). The retrieval of marine weathering records preserved by strontium stable isotopes in foraminifera. *EOS Trans. AGU 91* (Fall Meeting Suppl., Abstr. B21D–0343).
- Stevenson, E. I., Hermoso, M., Rickaby, R. E. M., Tyler, J. J., Minoletti, F., Parkinson, I. J., Mokadem, F., & Burton, K. W. (2014). Controls on stable strontium isotope fractionation in coccolithophores with implications for the marine Sr cycle. *Geochimica et Cosmochimica Acta*, 128, 225–235.
- Stevenson, R., Pearce, C. R., Rosa, E., & Hélie, J.-F. (2018). Weathering processes catchment geology and river management impacts on radiogenic ($^{87}\text{Sr}/^{86}\text{Sr}$) and stable ($^{88}\text{Sr}/^{86}\text{Sr}$) strontium isotope compositions of Canadian boreal rivers. *Chemical Geology*, 486, 50–60.
- Sun, H., Han, J., Zhang, S., & Lu, X. (2010). Chemical weathering inferred from riverine water chemistry in the lower Xijiang basin, South China. *Science of the Total Environment*, 408, 4749–4760.
- Sun, H., Liu, Z., & Yan, H. (2014). Oxygen isotope fractionation in travertine-depositing pools at Baishuitai, Yunnan, SW China: Effects of deposition rates. *Geochimica et Cosmochimica Acta*, 133, 340–350.
- Szramek, K., McIntosh, J. E., Williams, E. L., Kanduč, T., Ogrinc, N., & Walter, L. M. (2007). Relative weathering intensity of calcite versus dolomite in carbonate-bearing temperate zone watersheds: Carbonate geochemistry and fluxes from catchments within the St. Lawrence and Danube river basins. *Geochemistry, Geophysics, Geosystems*, 8, 26.

- Szramek, K., Walter, L. M., Kanduč, & Ogrinc, N. (2011). Dolomite versus calcite weathering in hydrogeochemically diverse watersheds established on bedded carbonates (Sava and Soča Rivers, Slovenia). *Aquatic Geochemistry*, 17, 357–396.
- Tang, J., Köhler, J. S., & Dietzel, M. (2008a). Sr²⁺/Ca²⁺ and ⁴⁴Ca/⁴⁰Ca fractionation during inorganic calcite formation: I. Sr incorporation. *Geochimica et Cosmochimica Acta*, 72(15), 3718–3732.
- Tans, P., Fung, I. Y., & Takahashi, T. (1990). Observational constraints on the global atmospheric CO₂ budget. *Science*, 247, 1431–1438.
- Tanweer, A., Gröning, M., Van Duren, M., Jaklitsch, M., & Pölsenstein, L. (2009). TEL Technical Note No. 43 Stable Isotope Internal Laboratory Water Standards: Preparation, Calibration and Storage. International Atomic Energy Agency, Vienna.
- Tchaikovsky, A., Häusler, H., Kralik, M., Zitek, A., Irrgeher, J., & Prohaska, T. (2019). Analysis of n(⁸⁷Sr)/n(⁸⁶Sr), δ⁸⁸Sr/⁸⁶Sr_{SRM987} and elemental pattern to characterise groundwater and recharge of saline ponds in a clastic aquifer in East Austria. *Isotopes in Environmental and Health Studies*, 55, 179–198.
- Teboul, P.-A., Durllet, C., Gaucher, E. C., Virgone, A., Girard, J.-P., Curie, J., Lopez, B., & Camoin, G. F. (2016). New perspectives provided by isotopic and geochemical tracers. *Sedimentary Geology*, 334, 97–114.
- Telmer, K., & Veizer, J. (1999). Carbon fluxes, pCO₂ and substrate weathering in a large northern river basin, Canada: Carbon isotope perspectives. *Chemical Geology*, 159, 61–86.
- Teng, F.-Z., Dauphas, N., & Watkins, J. M. (2017). Non-Traditional Stable Isotopes: Retrospective and Prospective. In *Reviews in Mineralogy & Geochemistry* (Vol. 82, pp. 1–26). Mineralogical Society of America.
- Tiwari, M., Singh, A. K., & Sinha, D. K. (2015). Stable isotope: Tools for understanding past climatic conditions and their applications in chemostratigraphy. In *Chemostratigraphy: Concepts, Techniques, and Applications* (pp. 65–92). Elsevier.
- Urey, H. C. (1947). The thermodynamic properties of isotopic substances. *Journal of Chemical Society*, 1, 562–581.
- Usdowski, E., Hoef, J., & Menschel, G. (1979). Relationship between ¹³C and ¹⁸O fractionation and changes in major element composition in a recent calcite-depositing spring—A model of chemical variations with inorganic CaCO₃ precipitation. *Earth and Planetary Science Letters*, 42, 267–276.
- Valley, J. W. (2001). Stable Isotope Thermometry at High Temperatures. *Reviews in Mineralogy and Geochemistry*, 43(1), 365–413.
- Vázquez-Urbez, M., Arenas, C., Sancho, C., Osácar, C., Auqué, L., & Pardo, G. (2010). Factors controlling present-day tufa dynamics in the Monasterio de Piedra Natural Park (Iberian Range, Spain): Depositional environmental settings, sedimentation rates and hydrochemistry. *International Journal of Earth Sciences*, 99, 1027–1049.
- Vollstaedt, H., Eisenhauer, A., Wallmann, K., Böhm, F., Fietzke, J., Liebetrau, V., Krabbenhoft, A., Farkaš, J., Tomašových, T., Raddatz, J., & Veizer, J. (2014). The Phanerozoic δ⁸⁸/δ⁸⁶Sr record of seawater: New constraints on past changes in oceanic carbonate fluxes. *Geochimica et Cosmochimica Acta*, 128, 249–265.
- Wang, H., Yan, H., & Liu, Z. (2014). Contrasts in variations of the carbon and oxygen isotopic composition of travertines formed in pools and a ramp stream at Huanglong Ravine, China: Implications for paleoclimatic interpretations. *Geochimica et Cosmochimica Acta*, 125, 34–48.
- Watkins, J. M., Hunt, J. D., Ryerson, F. J., & DePaolo, D. J. (2014). The influence of temperature, pH, and growth rate on the δ¹⁸O composition of inorganically precipitated calcite. *Earth and Planetary Science Letters*, 404, 332–343.

- Watkins, J. M., Nielsen, L. C., Ryerson, F. J., & DePaolo, D. J. (2013). The influence of kinetics on the oxygen isotope composition of calcium carbonate. *Earth and Planetary Science Letters*, 375, 349–360.
- Weijermars, R., Mulder-Blanken, C. W., & Wiegers, J. (1986). Growth rate observation from the moss-built Checa travertine terrace, central Spain. *Geol. Mag.*, 123, 279–286.
- Wohl, E., Hall, R. O., Lininger, K. B., Sutfin, N. A., & Walters, D. M. (2017). Carbon dynamics of river corridors and the effects of human alterations. *Ecological Monographs*, 87, 379–409.
- Yan, H., Liu, Z., & Sun, H. (2020). Large degrees of carbon isotope disequilibrium during precipitation associated degassing of CO₂ in a mountain stream. *Geochimica et Cosmochimica Acta*, 273, 244–256.
- Yan, H., Sun, H., & Liu, Z. (2012). Equilibrium vs. Kinetic fractionation of oxygen isotopes in two low-temperature travertine-depositing systems with differing hydrodynamic conditions at Baishuitai, Yunnan, SW China. *Geochimica et Cosmochimica Acta*, 95, 63–78.
- Zachos, J., Pagani, M., Sloan, L., Thomas, E., & Billups, K. (2001). Trends, rhythms, and aberrations in global climate 65 Ma to present. *Science*, 292, 686–693.
- Zavadlav, S., Kanduč, T., McIntosh, J., & Lojen, S. (2013). Isotopic and chemical constraints on the biogeochemistry of dissolved inorganic carbon and chemical weathering in the karst watershed of Krka river (Slovenia). *Aquatic Geochemistry*, 19, 209–230.
- Zavadlav, S., Mazej, D., Zavašnik, J., Rečnik, A., Dominguez-Villar, D., Cukrov, N., & Lojen, S. (2012). C and O stable isotopic signatures of fast-growing dripstones on alkaline substrates: Reflection of growth mechanism, carbonate sources and environmental conditions. *Isotopes in Environmental and Health Studies*, 48, 354–371.
- Zavadlav, S., Rožič, B., Dolenc, M., & Lojen, S. (2017). Stable isotopic and elemental characteristics of recent tufa from a karstic Krka River (south-east Slovenia): Useful environmental proxies? *Sedimentology*, 64, 808–831.
- Zhao, M., Zheng, Y., & Zhao, Y. (2016). Seeking a geochemical identifier for authigenic carbonate. *Nat Commun*, 7, 10885.
- Zhu, T., & Dittrich, M. (2016). Carbonate Precipitation through Microbial Activities in Natural Environment, and Their Potential in Biotechnology: A Review. *Frontiers in Bioengineering and Biotechnology*, 4:4. <https://doi.org/10.3389/fbioe.2016.00004>
- Zieliński, M., Dopieralska, J., Belka, Z., Walczak, A., Siepak, M., & Jakubowicz, M. (2017). The strontium isotope budget of the Warta River (Poland): Between silicate and carbonate weathering, and anthropogenic pressure. *Applied Geochemistry*, 81, 1–11.

Bibliography

Journal Articles

L. Rovan, T. Zuliani, B. Horvat, T. Kanduč, P. Vreča, Q. Jamil, B. Čermelj, E. B. Nakić, N. Cukrov, M. Štok, S. Lojen, [2021] “Uranium isotopes as a possible tracer of terrestrial authigenic carbonate.” *Science of the Total Environment* vol. 797, pp. 149103(1-12), 2021.

Conference Presentations

S. Lojen, Q. Jamil, T. Zuliani, L. Rovan, T. Kanduč, P. Vreča, M. Štok, E. B. Nakić, N. Cukrov, “Sr isotope fractionation in a karst river: case study of Krka, Croatia,” EGU General Assembly 2021, online, 19-30 April 2021, EGU21-6059.

S. Lojen, T. Zuliani, L. Rovan, B. Horvat, T. Kanduč, P. Vreča, Q. Jamil, M. Štok, “Uranium and strontium isotopes in recent and interglacial tufa in Krka National Park (Croatia),” *Goldschmidt2021*, 4-9 July 2021.

Biography

The author of this thesis, Qasim Jamil, was born in 1994 in Pakistan, where he obtained his Bachelor of Chemical Engineering in 2017 from the University of the Punjab, Lahore, Pakistan, one of the oldest and most renowned institutes in the country. He has been interested in the interdisciplinary research of Analytical Chemistry, Geochemistry and Environmental Sciences. Following his interest, he pursued his Masters in Ecotechnologies from Jožef Stefan International Postgraduate School, Ljubljana, Slovenia. His main area of interest during post-graduation studies is Environmental Chemistry.